Lignocaine Permeability through the Paraneural Sheath and Human Sciatic Nerve – A Study on In Vitro Biological Membrane and Nerve Model.

Synopsis of the thesis to be submitted for the award of the

DOCTOR OF PHILOSOPHY

Under the Faculty of Medicine

Submitted to

SRI BALAJI VIDYAPEETH

(Deemed to be University u/s 3 of UGC Act 1956)

Accredited by NAAC with 'A++' Grade

Pondicherry - 607402

By

Dr. T. Sivashanmugam. MD,DNB, PDCC, FRCP.

UIN: 1505001012

Under the guidance of

Dr. M. Ravishankar. MD, FRCP.

Director, C DREaMS, SBV.

Month and year of submission: May 2024

S. No	Contents	Page No.
1	Introduction	1-3
2	Aim and objectives	3
3	Research question	3
4	Review of literature	3 - 9
5	Methodology	9 - 24
6	Results	24 - 28
7	Discussion	28 - 33
8	Summary and conclusion	33
9	References	33 - 37

1. Introduction:

The therapeutic efficacy of any drug relies on its bioavailability at its site of action. In the case of any biological system, it is not always possible to deposit the drug at the effect site. Hence from the point of delivery to the effect site, the drug molecule must move across different biological barriers. These biological barriers are present in various sizes, shapes, and architecture. The spinal cord meninges in epidural drug delivery, paraneurium, epineurium, perineurium, and endoneurium during peripheral nerve blockade, fascial and muscular planes in compartment blocks are examples of biological barriers that offer varying impedance to the drug diffusion in the anaesthetic drug delivery paths. The influence of these biological barriers can be very well perceived in the latency and failures during clinical peripheral nerve blockade for surgical anaesthesia.

Even after the introduction of Ultrasound, complete conduction blockade of the plexus and peripheral nerve required injection of a relatively large volume and high concentration of local anaesthetic. During spinal anaesthesia, minimum effective anaesthetic concentration (MEAC) while using 48 mg dose of lidocaine was reported as 0.54%. Any concentration above this with the same dose of drug, produced same quality of surgical anaesthesia up to T12 level[1]. On the other hand, the expression changes to mean effective volume (MEV 90%) of the drug in a particular concentration while communicating about the plexus and peripheral nerve blocks. The total quantum of the drug increases to 10 folds, that is 480 mg, 32 ml of 1.5 % lidocaine was determined to be the MEV90 while performing ultrasound (US) guided supraclavicular brachial plexus block[2]. Although, the drug absorption by the systemic circulation and surrounding non-neural tissues uptake of LA is different between the two sites, this increased requirement of the local anaesthetic dose is essentially due to the diffusion barrier imposed by the multiple layers of connective tissues found around axons in the peripheral nerves[3]. These multiple layers of connective tissues are absent around the spinal rootlets inside the subarachnoid space. The in-vivo animal experiments unequivocally revealed that despite administering a high dosage of LA around the peripheral nerve, less than 2% of the injected mass was detected within the nerve during the complete functional blockade[4]. This indicates that for producing the desired clinical effect, the actual amount of LA needed inside the nerve is exceedingly small. Even though, corresponding human nerve tissue data is lacking, by comparing the requirement for local anaesthetics (LA) in subarachnoid and peripheral nerve block, we can deduce that the current injection techniques at the peripheral nerves and plexus blockade are highly

ineffective in delivering drugs to the intended site of action[5]. The preclinical research on the uptake and wash out kinetics of LA from the rat sciatic nerve concluded that perineurium could be the significant diffusion barrier during the peripheral nerve blockade[6]. In contemporary US guided regional anaesthesia practice, the current resolution of the US technology is unable to distinguish the perineurium within the nerve, but it is possible to clearly identify the paraneural sheath and subparaneural compartments surrounding the sciatic nerve[7] and components of the brachial plexus in the supraclavicular[8] and costoclavicular regions[9]. Depositing local anaesthetic within this subparaneural compartment, between paraneural sheath and epineurium, has shown to provide faster onset of conduction blockade and prolonged duration of analgesia[10,11]. However, the permeability of these para neural connective tissues to the local anaesthetic diffusion is unknown. Measuring the permeability of the human paraneural sheath to the local anaesthetics will yield crucial human data to understand the contribution of connective tissues around the peripheral nerve in the onset of surgical anaesthesia and potential block failures. Hence, we decided to measure the permeability of the paraneural sheath of the human sciatic nerve harvested from fresh postmortem specimens.

The in vivo studies provide limited information regarding the permeability of biological barriers because of unpredictable surface area exposure, systemic uptake, and local tissue absorption of study drugs. Hence in vitro studies are inevitable, where the surface area available for diffusion, concentration gradient across the membrane, and sink conditions can be standardized and maintained. Validated diffusion cells or chambers are the critical equipment needed for in-vitro permeation studies. Even though numerous permeation devices are commercially available, the vertical Franz diffusion cell (FDC) is the most studied and recommended by FDA (Food and Drug Administration) and OECD (Organization for Economic Co-operation and Development)[12, 13]. Unfortunately, their application is well established for testing semi-solid dosage forms in skin permeation studies. However, analyzing the permeability of biological membranes required drugs in solution form on either side of the membrane with uniform mixing without any leak and a stable temperature environment in both chambers. Commercial cells satisfying all these requirements are infrequent [14]. Hence many authors utilized customized diffusion chambers for their studies on biological membranes[15-17]. Since, the commercially available Franz diffusion cell did not meet our experimental requirements, we designed this in-vitro study in two steps. Step 1. To design, develop and validate a novel diffusion cell that meets our

experimental setup requirements. Step 2. To measure the Lignocaine permeability of the human Para neural sheath utilizing the novel diffusion cell and to measure the Lignocaine uptake of the human sciatic nerve without the paraneural sheath.

2. Aim and objectives:

Aim:

To determine the Lignocaine permeability of Para neural sheath and Lignocaine uptake of human sciatic nerve without the paraneural sheath in vitro settings.

Objectives:

1. To design, develop and validate a novel diffusion cell that satisfy the current experimental setup requirements.
2. To procure human sciatic nerve from fresh cadavers (post mortem specimens), separate the paraneural sheath and the nerve, mount the paraneural sheath into the novel diffusion cell and measure the Lignocaine permeability. To measure the Lignocaine uptake of human sciatic nerve without the paraneural sheath separately.

3. Research questions:

1. What is the Lignocaine permeability of the paraneural sheath of the human sciatic nerve and the lignocaine uptake of the de-sheathed nerve?

4. Review of literature:

4.1 The design of Diffusion Cell or Chambers utilised for the in vitro permeability studies in the past.

Since as early as 1982, Moore et al [18] measured the Dural permeability to narcotics in vitro settings. They designed and built a customized diffusion cell at the Nuffield Department

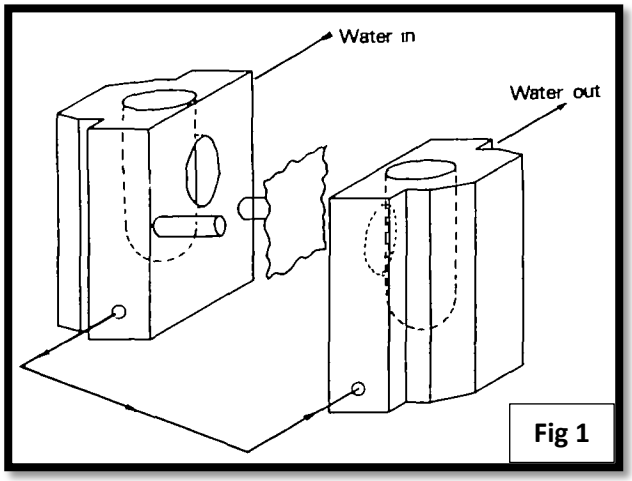

Anaesthetics, John Radcliffe Hospital, Oxford. This cell consisted of two Perspex blocks each with a chamber of similar shape and volume (10 ml each) which clamped together so that the chambers communicated through a circular port of fixed area (2.82 cm^2). The entire device was kept at a given temperature – controlled water bath (Figure 1) with a magnetic stirrer was placed inside the chambers throughout the procedure. In 1990, Bernards CM et al. [19] used their customized diffusion cell made up of Plexiglass to measure the meningeal permeability of morphine and alfentanil. In their setup they placed the all three meninges in their normal anatomical relationships between two halves of the temperature controlled diffusion chambers with a 0.785 cm^2 connecting port (Figure 2). Chamber volume was filled with 10 ml of buffered mock CSF solution and both the chambers were stirred with magnetic stirrer. Bernard et al used the same diffusion cell to measure the permeability across spinal root sleeve in 1991[20], physical and chemical properties of drug molecules governing their diffusion through the spinal meninges in 1992[21], effect of needle puncture on morphine and Lidocaine flux through the spinal meninges of monkey in vitro in 1994[22], later influence of palmitoyl carnitine on trans meningeal flux on hydrophilic drugs in 1996[23]. While Bernard et al. used their Plexiglass custamized diffusion cell for their in vitro permeation studies, in 1992 Richard F. McEllistrem [16] utilised their own diffusion chamber to study the permeability of the human dura mater to opioid and local anaesthetics. The device was made up of two glass chambers A and B (Figure 3). These chambers were fitted tightly together by means of a locking clamp and O- ring to form a tight seal. The surface area of the connecting port was approximately 3 cm^2 . Each chamber contained 5 ml of artificial cerebrospinal fluid (CSF) at pH 7.4 for opioid

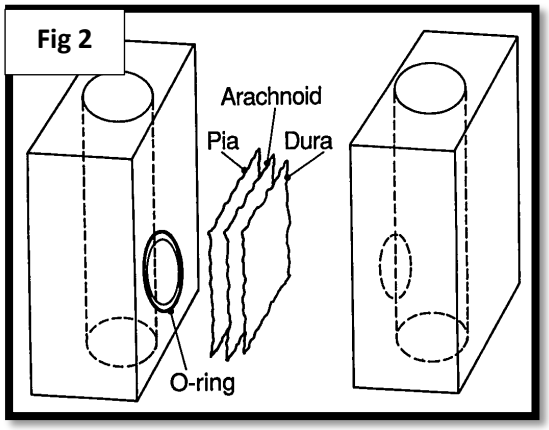

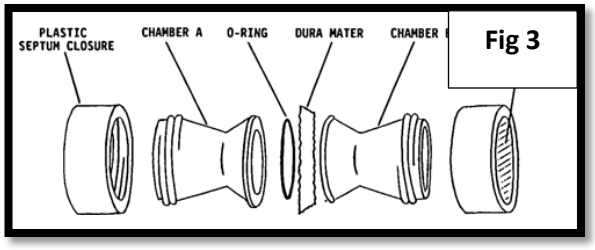

compounds and pH 6.8 for local anaesthetic compounds to prevent precipitation. Specially prepared disposable Sylgard SEPTA were fitted to the ends of each chamber, held in place by black phenolic screw caps with open tops. A sample of test drug solution was introduced into chamber A at time zero and 50 micro litter aliquots were withdrawn from chamber B at predetermined intervals of 0, 20, 40, 60, 120, and 180 mins using a Hamilton syringe. The contents were continuously mixed by means of a Burrell wrist action shaker (Burrell Scientific In, PA USA) and all experiments were performed at room temperature. In 2000, Rene Grouls et al. [24] used Borosilicate glass diffusion cell (Product details and the image of the device was not provided) . The diffusion cell consisted of two chambers of 50 ml capacity. The connecting port had an effective diffusion area of 1.43 cm . The compartments were surrounded by water jackets and kept at a temperature of 37° C during experiments. Both chambers were filled with 50 ml of thermostatic Phosphate Buffered Saline (PBS) at 37° C. The solutions in both compartments were constantly stirred by Teflon- coated magnetic stirrer bars (100 rpm). In 2004, Rozenn clement et al. [25] utilized a different Plexiglass thermostatic diffusion cell to measure the Dural permeability of rabbits in ex vivo settings. The diffusion cell had an effecting diffusion area of 0.6 cm^2 with a chamber volume of 8ml. (Image of the diffusion cell was not provided, Product could not be accessed in commercial search). Considering the limitations and infrequent availability of the previous diffusion cells, Karsnov et al[17] in 2017 proposed a new diffusion cell made up of 2 reservoirs with a 6mm connecting port for diffusion across the chambers. Plastic cuvette for spectrophotometers (10×10×45mm) were used as the reservoirs. The reservoir volume was 2 ml each. Both the chambers were attached together with help of adhesive plasters (Figure 4). They tested the permeability of spinal cord dura mater of dogs for varying substances present in the blood serum and shown that the results were reproducible. Thus no

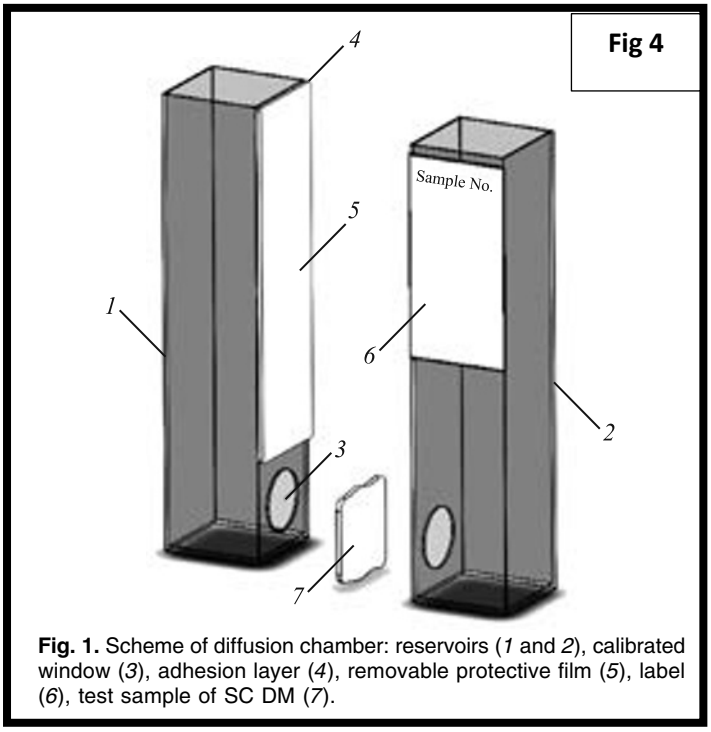

Fig. 1. Scheme of diffusion chamber: reservoirs (*1* and *2*), calibrated window (*3*), adhesion layer (*4*), removable protective film (*5*), label (*6*), test sample of SC DM (*7*).

two researchers utilized the same diffusion cell with the same experimental set up like chamber volume, composition of study solution, stirring speed, effective diffusion area etc. Apart from the standard Franz Diffusion Cell, the described cells in the literature were not easily available through the commercial market and there was no mention of validation of the customized diffusion cells. Hence we were forced to design and validate a novel diffusion cell that suites our biological membrane and experimental needs.

4.2 Review of existing literature on Lignocaine permeability of the human paraneural sheath and lignocaine uptake into human sciatic nerve.

Currently we don't have any literature on lignocaine permeability of human paraneural sheath and lignocaine up take into the human sciatic nerve. We have lignocaine permeability data for human [16, 24] as well as animal spinal cord meninges [21]. The lignocaine uptake data is available only for isolated nerve segments of animal origin. [4,5, 26-28]

4.2.1 Lignocaine permeability of human and animal spinal cord meninges.

McEllistrem et al[6] in 1992 attempted to measure the lignocaine permeability of human dura mater in vitro settings. They harvested 3 to 4 cm sections of human dura mater, from 13 subjects at post-mortem examination and dry frozen at – 70^{o} Celsius. At a later date they have conducted the permeation experiment through a customized diffusion cell. The Dural specimens were placed between the ports (area = 3 cm2) of two glass chambers A and B (Figure 3). Each chamber contained 5 ml of artificial cerebrospinal fluid. 0.1% (1000 µgm/ml) Lignocaine was introduced into chamber A and 50 µ1 aliquots of mock CSF were withdrawn from the other chamber B at predetermined intervals. They determined the permeability by calculating the rate of diffusion (slope) from the plot of mean drug concentration (chamber B) versus time and found that the lignocaine permeability of the human dura was 1.024 ± 0.051µgm/ml/min (mean ± SEM). They have concluded that the Dura mater permeability was shown to be a simple diffusion process and to be independent of lipid-solubility and molecular weight. Permeability appeared to increase with age and may have a linear relationship to the initial concentration. Their methodology and calculation of permeability was criticized by Bernard et al[29] on three aspects 1. Without analysing the permeability of Dura and Arachnoid mater separately they concluded that the principle diffusion barrier was Dura mater. 2. The slope of mean drug concentration in the recipient chamber indicated the Flux that is mass movement of the drug in per unit time

across the available surface area which is concentration dependant rather than permeability which is a constant that takes concentration gradient into account. 3. Unknown effect of cold storage of the biological tissues and its permeability characterises. In the same year (1992) Bernard et al[21] in an experiment exploring the physical and chemical properties of drug molecules governing their diffusion through the spinal meninges measured the meningeal permeability of lignocaine in monkeys. They have placed all three layers of the meninges in their normal anatomical relationships placed between the two halves of a temperature controlled Plexiglass diffusion cell with a 0.785 cm 2 connecting port (Figure 2). 10 ml of bicarbonate buffered mock CSF was placed in the fluid reservoirs on either side of the meningeal tissue. At time 0, the study drug was added to the dura side of each tissue specimen (reservoir 1). Thereafter at 5 min intervals for 45 minutes, 200 µl samples were removed from reservoir 1 and reservoir 2 for drug concentration analysis. The mean Lignocaine permeability coefficient of 5 permeation experiments was 1.45 ± 0.12 cm / min × 10 – 3 . Rene Grouls et al[24] in 2000 measured the Diffusion of n-butyl-p-aminobenzoate (BAB), lidocaine and bupivacaine through the human dura–arachnoid mater in vitro. Approximately 2 × 2 cm specimens of dorsal meninges form T1 and T12 segments were harvested from 14 human beings during post mortem. The specimens were immediately stored in Phosphate Buffered Saline (PBS) at – 20º C and thawed later for permeation experiments. The meningeal tissues were mounted in a borosilicate glass diffusion cell. The diffusion cell consisted of two compartments of 50 ml each. The connecting port had an effective diffusion area of 1.43 cm2 . The compartments were surrounded by water jackets and kept at a temperature of 37º C during experiments. Both chambers were filled with 50.0 ml of thermostated PBS at 37º C. First the receiver compartment was filled with 50.0 ml plain PBS; 5 min later, to assure integrity of the meninges by visual inspection on leakage, 50.0 ml of 0.1% Lignocaine HCL in PBS solution (PH 7.4) was placed in the donor compartment (dura side). The solutions in both compartments were constantly stirred by Teflon- coated magnetic stirrer bars (100 rpm). The concentration of the local anaesthetic in the receiver compartment was measured during 30 min at 3 min intervals in a quartz flow-through cell by UV-spectrometry (Beckman DU 7500; Beckman Instruments, Fullerton, USA). Absorbance was measured in triplicate (middle measurement at indicated time) at the maximum of UV absorption (fixed wavelength BAB 287 nm; bupivacaine 263 nm and lidocaine 264 nm). The (mean ± S.E.M; n = 6) Lignocaine permeability at T1 was significantly (p = 0.003) less (17.7 ± 1.4 vs 24.2 ± 2.6 × 10 – 3 cm / min) than at T 12

segment. Similar pattern of less permeability was observed in Bupivacaine at T1 level when compared to the T12 level (26.7 ± 4.2 vs 34.7 ± 5.9 × 10 – 3 cm / min). The permeability difference between the two spinal cord level was attributed to the thickness of dura at these levelsthe thickness being 0.45mm at thoracic compared to 0.3mm at Lumbar level.

4.2.2 Lignocaine uptake of animal sciatic nerve with or without the sheath.

In the past Lignocaine uptake into the sciatic nerve experiments were conducted both in vivo as well as in vitro settings.

4.2.2.1 Invitro local anaesthetic nerve uptake experiments.

In 2013, Stanley Leeson and Gray Strichartz[5] conducted in vitro experiments to investigate the kinetics of lignocaine uptake and washout in the rat sciatic nerve. In one set of experiments, they exposed sheathed rat sciatic nerves to a 1% lignocaine solution dissolved in 0.9% NaCl buffered with 5mM piperazine-N,N′-bis[2-ethane-sulfonic acid] (PIPES, Sigma), adjusted to a pH of 6.8 to 6.9 with NaOH (Pipes Buffered Saline -PBS). The nerves were exposed to lignocaine for 3 hours at 37°C. At various time points, the nerves were removed and desheathed, and both the sheath and nerve were separately assayed for lidocaine content. Their findings indicated that the time constant for sheath uptake was 6.7 ± 2.7 minutes (mean ± SD), while for nerve uptake, it was 27.4 ± 15.9 minutes ($P < 0.01$). The equilibrium uptakes ($L\infty$) were 49.0 ± 2.9 nmoles/mg wet for the sheath and 43.8 ± 7.2 nmoles/mg wet for the nerve ($P > 0.05$). To assess the influence of the epineural sheath on lignocaine uptake into the nerve, they examined the uptake kinetics of 0.2% (7.4mM) lignocaine in PBS into ensheathed and desheathed nerves. The former had their epineuria removed after incubation, while the latter were microsurgically stripped of their epineuria before incubation. Analysis revealed that the equilibrium uptakes were the same ($L\infty$ = 21.6 ± 3.6 mg wet tissue in ensheathed nerves and 17.2 ± 2.8 mg/wet tissue in desheathed nerves, $P > 0.05$). However, uptake was approximately half as fast in the ensheathed nerve, with a time constant of 9.1 ± 4.7 minutes, compared to the desheathed nerve, with a time constant of 5.3 ± 2.9 minutes ($P < 0.02$). Thus, they concluded that the epineural sheath presented some obstacle to the entry of lignocaine into the nerve. Based on another set of experiments, they also concluded that the neural content of lidocaine increases proportionately to its concentration in the incubation solution, up to approximately 5 to 10 mM (0.14%–0.28%), when uptake begins to saturate. In the linear range, neural uptake corresponds to a

partitioning coefficient (slope) of approximately 3.5 nmoles/mg rat nerve/mM lidocaine in the bathing solution. Comparable results were reported by other authors from studies on isolated nerves. Rosenberg et al[30]. found that ensheathed rat sciatic nerves exposed to 1 mM lidocaine took up 1.4 nmoles/mg wet nerve, while Strobel and Bianchi et al[31]. measured 1.5 nmoles/mg wet of toad sciatic nerve incubated in 0.5 mM lidocaine.

4.2.2.2 In vivo local anaesthetic nerve uptake experiments.

The concentration of neural lidocaine content observed in vivo following sciatic nerve block is notably lower compared to the in vitro experiments. Popitz-Bergez et al[4]. measured a range of 8 to 10 nmoles/mg of wet nerve tissue in the nerve segment closest to the injection site of 0.1 mL containing 1% (37 mM) lidocaine at pH 6.8, during the time of maximal conduction blockade. Nakamura et al[27]. detected neural contents ranging from 1 to 6 nmoles/mg of wet tissue using 0.05 to 0.2 mL of 0.5% lignocaine (pH 6.8). Similarly, Sinnott et al[32]. found a peak lidocaine content of 10 to 11 nmoles/mg of wet tissue with 0.5% lignocaine at pH 7.8, suggesting enhanced drug penetration from a more alkaline solution. These observations indicate that the neural content of local anesthetics (LA) ranges from 1 to 10 nmoles/mg of wet nerve tissue under in vivo conditions, in contrast to the 33 or 40 nmoles/mg of wet tissue observed for the same doses of 0.5% and 1% lidocaine, respectively, under in vitro conditions. This disparity is attributed to systemic absorption of local anesthetics from both extraneural (via the vasculature) and intraneural sources (via intraneural vascular uptake), as well as uptake by surrounding non-neural tissues.

5. Materials and methods:

5.1. Objective 1: To design, develop and validate a novel diffusion cell that satisfy the current experimental setup requirements.

5.1.1 : The ideal diffusion cell requirements for the current experimental setup.

1. The diffusion cell should allow a large enough surface area (minimum of 1 cm^2) for the diffusion to take place effectively.
2. High surface area for diffusion and minimal chamber volume (High surface area to volume ratio) enables effective measurement of less diffusible agent like local anaesthetics.

3. Apart from the membrane characteristics no other factors like gravity, unstirred water layers, air bubbles near the diffusion surface should influence the permeation of the study drug.
4. The leak in the diffusion chamber should be less than 5%.
5. Longitudinal orientation of the diffusion port is ideal to match the longitudinal architecture of the paraneural sheath of the human sciatic nerve.
6. Sampling volume should not affect the diffusion dynamics.
7. Temperature of the cell should be maintained at a constant temperature.
8. The solutions at both the chambers should be stirred continuously to prevent the settling of the drug at the bottom due to gravity creating unstirred water layer.
9. Repeated sampling should not create air bubbles near the diffusion surface.
10. The volume of donor and the recipient chamber should be equal so that both the compartments can be filled at the same time interval.

5.1.2 Design and Development

Many prototype drawings were done to satisfy the requirements of a above mentioned ideal diffusion cell. After several brainstorming sessions and modifications of the drawing, the design was finalized to be a **S**tatic, **h**orizontally **a**lig**n**ed **D**rug **D**iffusion **C**ell (Shan DDC) as shown in the Figure 5.

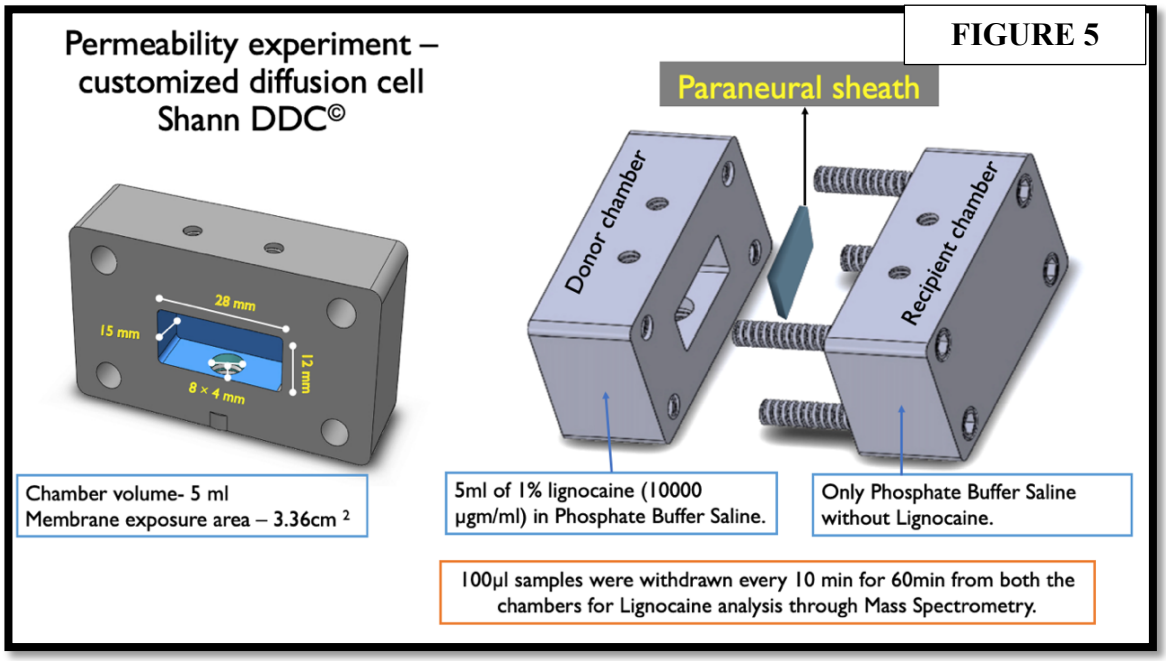
FIGURE 5
Permeability experiment – customized diffusion cell Shann DDC©
Paraneural sheath
Donor chamber
Recipient chamber
28 mm
15 mm
12 mm
8 × 4 mm
Chamber volume- 5 ml
Membrane exposure area – 3.36cm ²
5ml of 1% lignocaine (10000 µgm/ml) in Phosphate Buffer Saline.
Only Phosphate Buffer Saline without Lignocaine.
100µl samples were withdrawn every 10 min for 60min from both the chambers for Lignocaine analysis through Mass Spectrometry.

The diffusion cell consists of a donor and a recipient chamber engraved separately in two polyacrylate blocks measuring 40 × 80 × 23 mm in length, width, and thickness

respectively. The diffusion chambers are in rectangular shape measuring 28 × 12 ×15 mm in length, width, and thickness respectively to hold a volume of 5 mL separately in each chamber. The membrane surface area available to facilitate the diffusion of molecule between the donor and recipient chamber is 3.36 cm^2. The chambers are held together facing each other by a helical screw thread system with the membrane in between that itself will act as a gasket and prevents leakage of the testing solutions. An 8 mm diameter and 4 mm depth well have been tapped into the floor of each chamber to accommodate a magnetic stirrer bead of appropriate size to ensure uniform mixing of solution in both the chambers. Two 2 mm diameter port have been drilled into the roof of the chambers to provide access for study drug delivery and sample withdrawal for analysis. The dimension of both the chambers are same, hence both can be utilized as donor or recipient cell.

The Shan-DDC was produced using SOLIDWORKS® 3D CAD software (Dassault Systemes, Vélizy-Villacoublay, FR). The geometry of the diffusion cell was optimized and the computer numerical control (CNC) program for the same was generated using Mastercam 3D (CNC Software Inc., Tolland, CT, USA). The prototype of the diffusion cell was engraved in the polyacrylic block using CNC machine (Makino, SG) fed with the Mastercam 3D information. Milling direction, feed rate and spindle speed were optimized for the surface quality of the material. The ports were created using a drill press to facilitate sample retrieval and drug additions. The dimension of the donor and recipient chambers of the diffusion cell was set to hold a maximum volume of 5mL each. Five such Shan-DDC were made to test the repeatability and for validation.

5.1.3 Validation of Shan-DDC

The performance of the Shan-DDC was validated against the established study parameters[33] like temperature stability, leak fraction and stirrer efficiency. The diffusion function of cell was tested by analyzing the Lignocaine Flux (Proposed LA for the Paraneural sheath permeability) across the cellulose nitrate synthetic membrane. Five experiments were performed in 5 different Shann-DDC on five different days under the same experimental conditions. Less than 10% coefficient of variation of Lignocaine Flux between the five experiments would indicate satisfactory reproducible device function towards in vitro permeation studies.

5.1.3.1 Leak testing

This was done in two settings.

1. The blocks were assembled with a nitrocellulose membrane mounted in-between, and the helical screws were tightened to maximum. The two chambers were filled with distilled water to the maximum and weighed with digital weighing balance. The cells were left to stand for 4 hours in room temperature and weighed again. The change in the gross weight of the diffusion cell before and after revealed the leak volume in milligrams. A multiplicative factor was used to convert the milligram to a microliter (100 microliters of distilled water = 0.098mg).
2. Leak fraction assessment in actual experimental condition

Before the start of experiment all components Shan-DDC, nitrocellulose membrane, and distilled water were incubated in a servo-controlled water bath for 30 minutes to reach 37°C. After incubation, the Shan-DDC was assembled by placing membrane in between chambers. 5mL of distilled water was then added in each chamber through a sample injection port. The gross weight of all the components of Shan-DDC with the distilled water was measured using a digital weighing balance (Sartorius, Gottingen, DE) to note the weight of the liquid before the experiment. After measuring the loaded diffusion cell weight, the cell was wrapped with water-proof cling drape and was immersed in a water bath set at 37°C, and the magnetic stirrer was set to rotate at 200rpm for 60 minutes. After 60 minutes of incubation, the diffusion cell was taken out and the cling drape and water droplets on the surface were removed and dried completely before weighing. The change in the gross weight of the diffusion cell before and after the incubation revealed the leak volume in milligrams. A multiplicative factor was used to convert the milligram to a microliter (100 microliters of distilled water = 0.098mg). less than 5% leak volume considered to be most ideal for many experimental setups.

This experiment was repeated on all 5 days without altering the experimental settings. The mean leak fraction of the 5 experiments was estimated to be 162 ± 45 microliters amounting to 1.62 % of the total chamber volume of 10ml (Donor + Recepeint).

5.1.3.2 Temperature stability measurements

To record donor and recipient chamber temperature fluctuations, customized temperature probe tips were introduced through their sampling ports and coupled to a digital hygrometer (HTC -1, Temperature humidity meter). The diffusion cell was subjected to the same experimental condition as described in previous section 5.1.3.1 (section 2). The temperature was recorded every five minutes of one-hour incubation.

The temperature maintenance experiments revealed both the donor and recipient chambers could maintain the temperature within a narrow range of $37^0 \pm 1.2^0$ C throughout the experiment period (Figure 6)

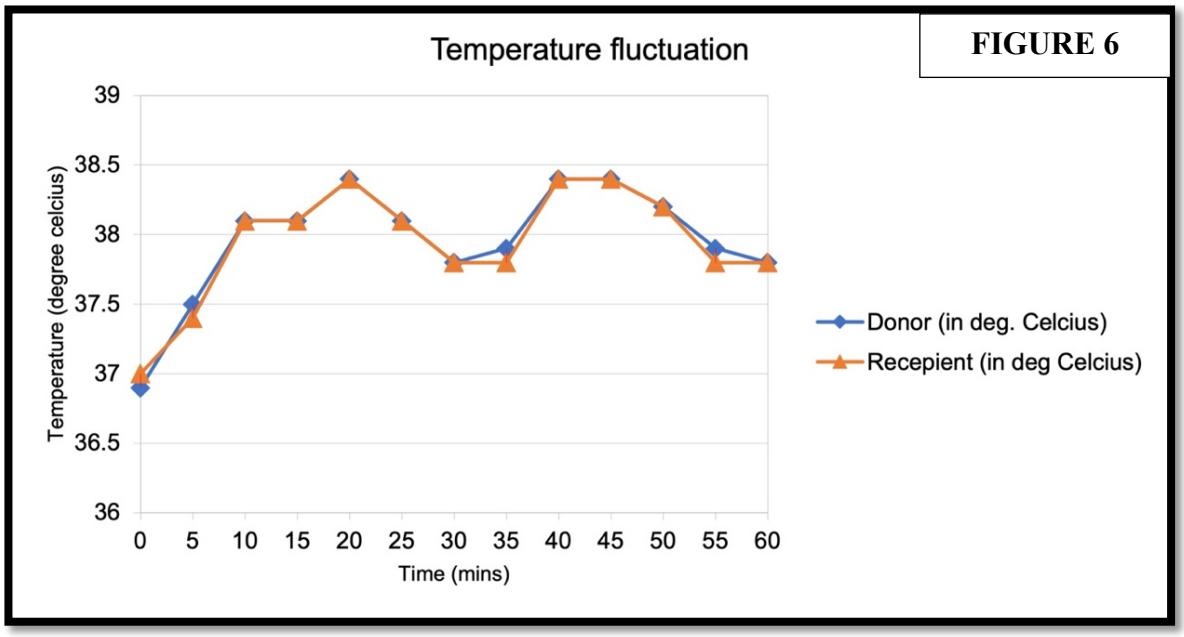

5.1.3.3 Measurements of stirrer efficiency using dye spread.

The dye colour spread in the donor and receptor chambers was used to assess the influence of stirring on sediment-free drugs distribution in the solution. The well on the bottom of the two chambers held a 2 × 5mm Poly-tetrafluoroethylene (PTFE)-coated micro magnetic stir bar (Tarsons Pvt. Ltd, Kolkata, IN). The Shan-DDC was filled with 5 mL of distilled water in the donor and recipient chambers and subjected to the experiment as described in section 5.1.3.1 (section 2). A video camera filmed dye mixing while five milligram of potassium permanganate crystals were introduced into the donor and recipient chambers one at a time. Two independent reviewers agreed on three parameters after reviewing the recording. 1. Colour dispersion time. 2. Sign of Vortex formation 3. Colour gradient within the chambers.

The 2 × 5mm micro magnetic bead at 200rpm offered effective stirring inside both the chambers and the mean time to uniform dye color spread to the entire cell was 36 ± 14 seconds and there was no vortex formation in any of the experiments (Figure 7).

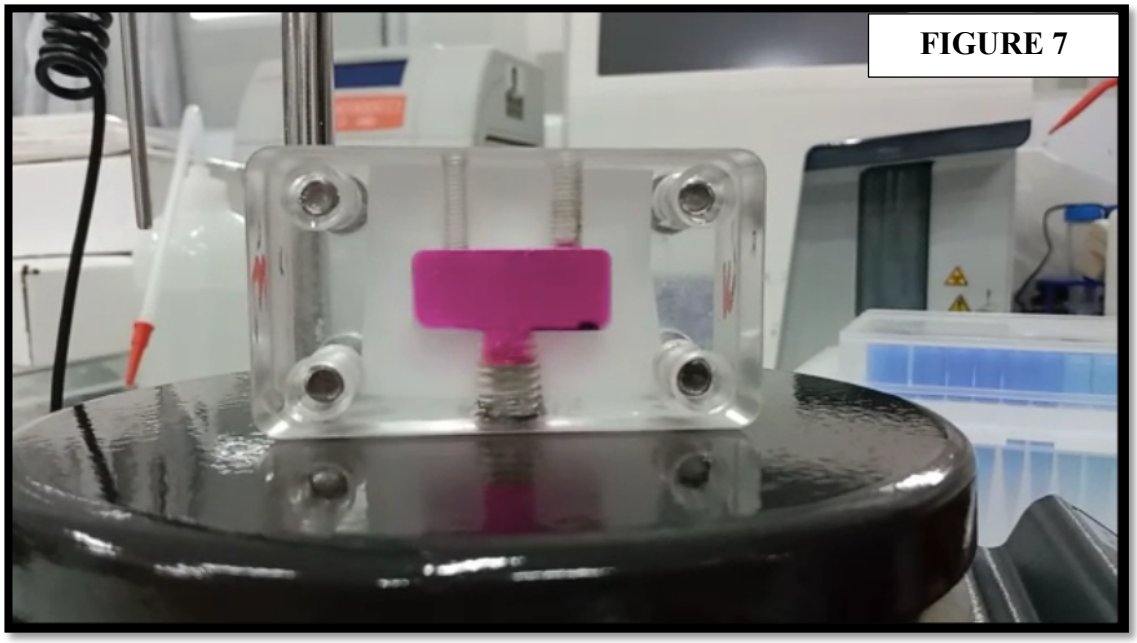

FIGURE 7

5.1.3.4 Diffusion function analysis

Since the aim was to study the permeability of paraneural sheath to Lignocaine, we had used the same Lignocaine to validate diffusion function of the Shan-DDC. A fresh 1% lignocaine solution was prepared by dissolving Lignocaine hydrochloride in the distilled water. Purchased lignocaine Hydrochloride I.P. had substance test purity of 99.67% W/W. (Suyog Pharmaceuticals Pvt. Ltd, Mumbai, IN). A 0.45 nm pore size cellulose nitrate membrane (Cole-Parmer India Pvt. Ltd, Mumbai, IN) was pre-treated with distilled water and placed between the donor and recipient chambers. The donor and the recipient chambers were filled with 5 mL of 1% lignocaine in distilled water and only distilled water respectively and subjected to the same experimental conditions as described in 5.1.3.1 (section 2). From the donor and the recipient cells, a sample of 100 µL was drawn through the sample retrieval port at 0, 15, 30, 45, and 60 minutes of incubation. The lignocaine concentrations were analyzed using SHIMADZU-SPD-20A series High-Performance Liquid Chromatography (HPLC) (Kyoto, JP).

5.1.3.5 Flux measurement and statistical representation

Lignocaine Flux (Q) was calculated by plotting the drug concentration data from the recipient chamber against time. The lignocaine flux through the cellulose nitrate membrane corresponds to the slope of the line relating concentration vs. time, as measured by least–squares linear regression. The slope was divided by the exposed membrane surface area to calculate the flux per 1 cm^2 of cellulose nitrate membrane, which was then multiplied by 60 to obtain the rate of drug diffusion across the membrane in one hour. Consequently, the

mean slope of all five experiments was obtained, and the coefficient of variation (CV%) between the slopes were calculated using the method Standard Deviation / Mean * 100. The average cumulative amount of lignocaine diffusion over a period of one hour through the nitrocellulose membrane was depicted in (Figure 8).

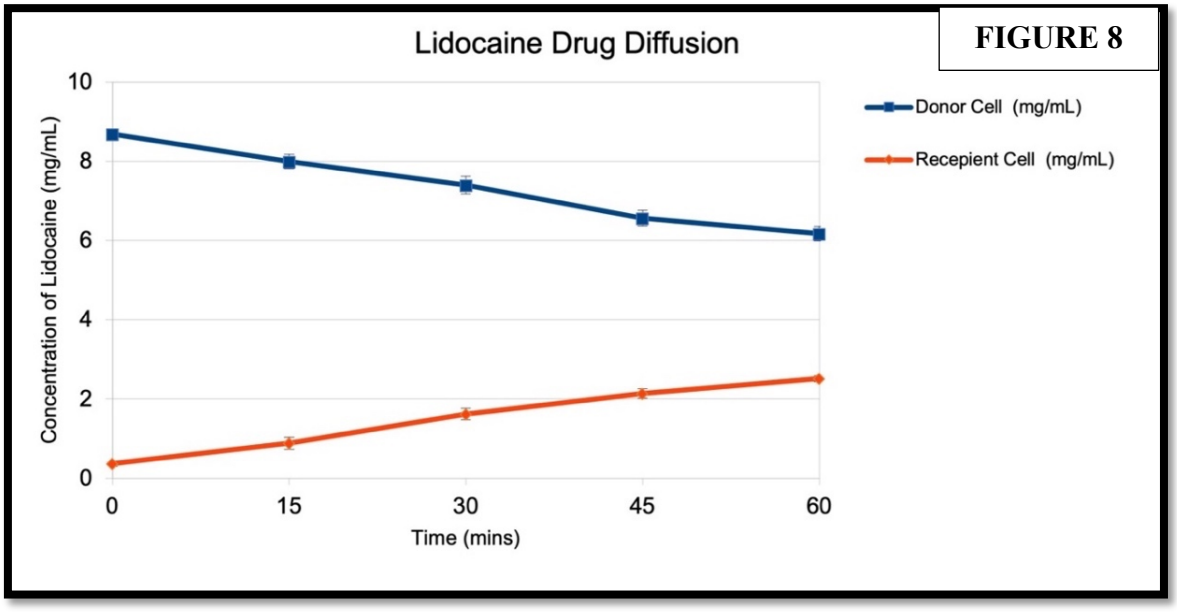

FIGURE 8

The identified steady state exhibited a good linear fit (r = 0.98). The mean lignocaine flux derived from the steady state slope of 5 plots was 0.67 ± 0.02 mg/cm^2/hr and the Coefficient of variation (CV) was 4.2% (Table 1).

Table 1 Validation of Lignocaine diffusion function of Shan-DDC through nitrocellulose membrane.

Experiment. No	Diffusion slope	Diffusion per cm^2 of the membrane	Lignocaine flux per hour	Mean flux	Standard deviation	% CV
1	0.0357	0.0108	0.6497	0.6735	0.02834	4.2087
2	0.0358	0.0108	0.6509			
3	0.0394	0.0119	0.7164			
4	0.0365	0.0111	0.6630			
5	0.0378	0.0115	0.6873			

5.2. Objective 2 methodology: Estimation of Lignocaine permeability of the paraneural sheath from human sciatic nerve.

5.2.1 Harvesting of the sciatic nerve from post mortem specimens.

This study was approved by PhD Research Advisory Committee (RAC) and Institute Human Ethics Committee of Sri Balaji Vidyapeeth Deemed to be University (Project no: PhD project/2017/04/01). 26 sciatic nerve specimens were harvested during post mortem examination from 13 diseased individuals with in 24 hours after their death . Informed consent was obtained from all the legal guardians of the deceased individuals (No.17/IHE/IGMC/F-7/2017/92). All the fresh cadavers were aged between 20 to 45 years. Individuals who suffered from lower limb infection, sepsis, burns, multi-organ dysfunction syndrome, and severe peripheral nervous system illnesses were excluded. After completing the routine post mortem examination, the cadavers were turned prone and a vertical skin incision was made over the posterior aspect of the mid-thigh starting from the sub gluteal region to the midpoint of the popliteal fossa. The incision was deepened with surgical blade with the help of self-retaining skin retractors. As the hamstring muscles were encountered, they were split apart with the re application of retractors. The sciatic nerve was commonly located as a white glistening structure beneath the bulk of semitendinosus and semi membranous muscles (Figure 9).

The sciatic nerve was completely exposed from the surrounding epimysium with the help of babcock forceps and fine surgical scissors (Figure 10).

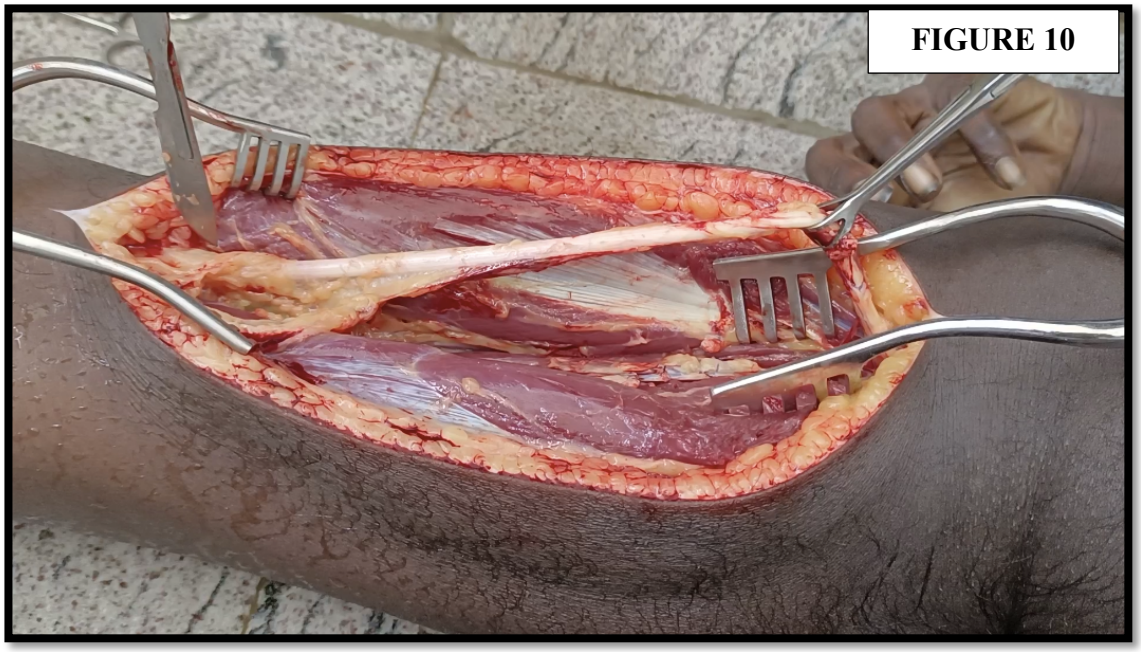

Care was taken not to injure or hold the paraneural sheath. After isolation approximately 15 cm length of the sciatic nerve was excided extending from the sub gluteal region to the post bifurcation. The collected sciatic nerve specimen was immediately placed into a container filled with Phosphate Buffered Saline and transported to the experimental laboratory immediately.

5.2.2 Separation of the membrane

Upon arrival, within one hour after removal from the body the paraneural sheath was dissected from the sciatic nerve through the microsurgical instruments. The sciatic nerve was placed on a custom-made glass plate and examined under 4X magnification through a surgical loop for any obvious physical damage to the paraneural sheath and the sciatic nerve. Then the paraneural compartment was opened with a microsurgical scissor and sequential dissection of the paraneural sheath was accomplished by a surgical blade (Figure 11, 12).

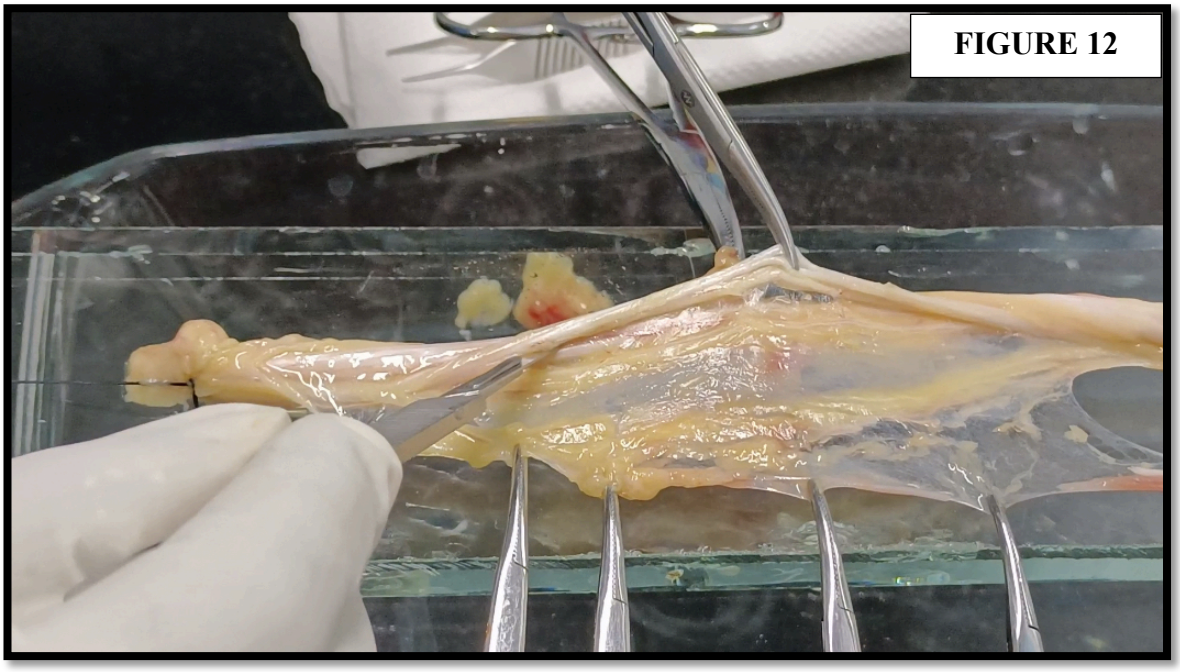

After a sizeable paraneural sheath had been dissected (40*80 mm), one half of the Shann DDC, which had been pre-incubated to 37 degrees Celsius in a servo-controlled water bath, was positioned beneath the sheath (Figure 13).

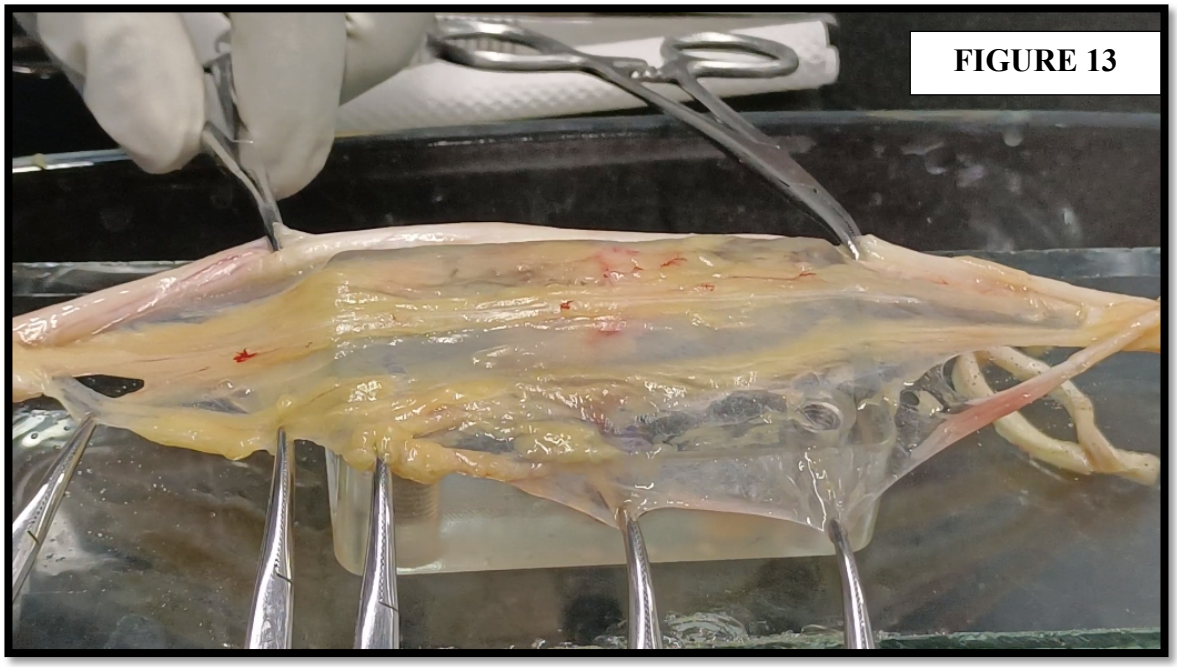

The other half of the Shan-DDC was then mounted on top of the sheath and secured using the helical screw thread system (Figure 14).

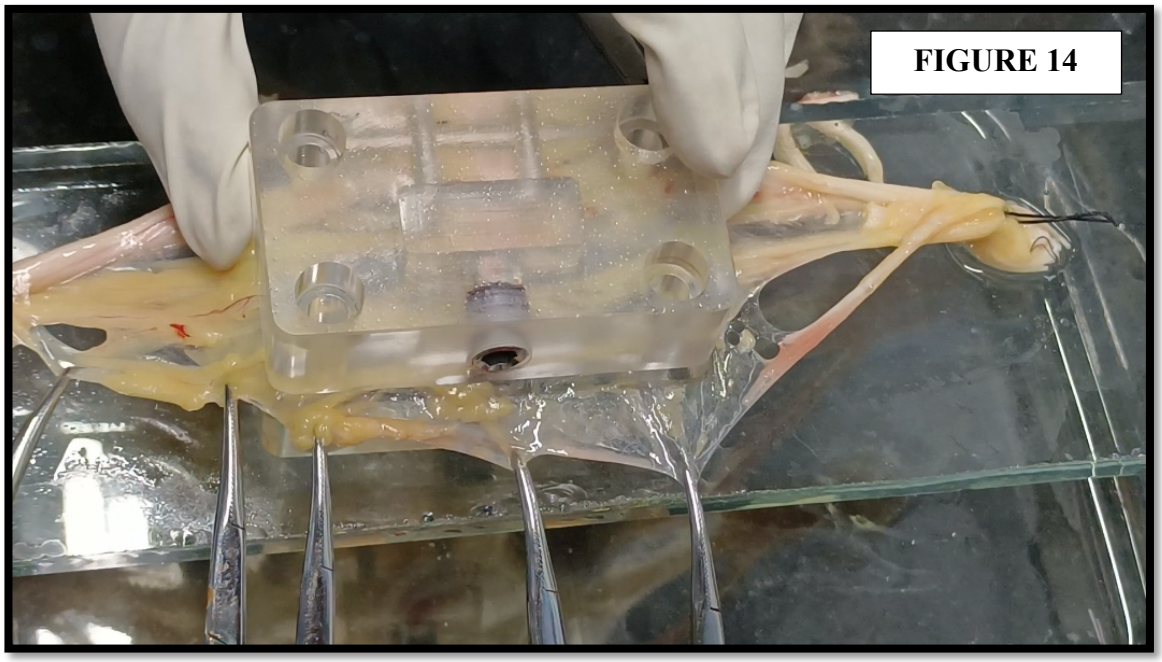

Then the paraneural sheath was cut all around the device, and the diffusion cell was detached from the nerve (Figure 15).

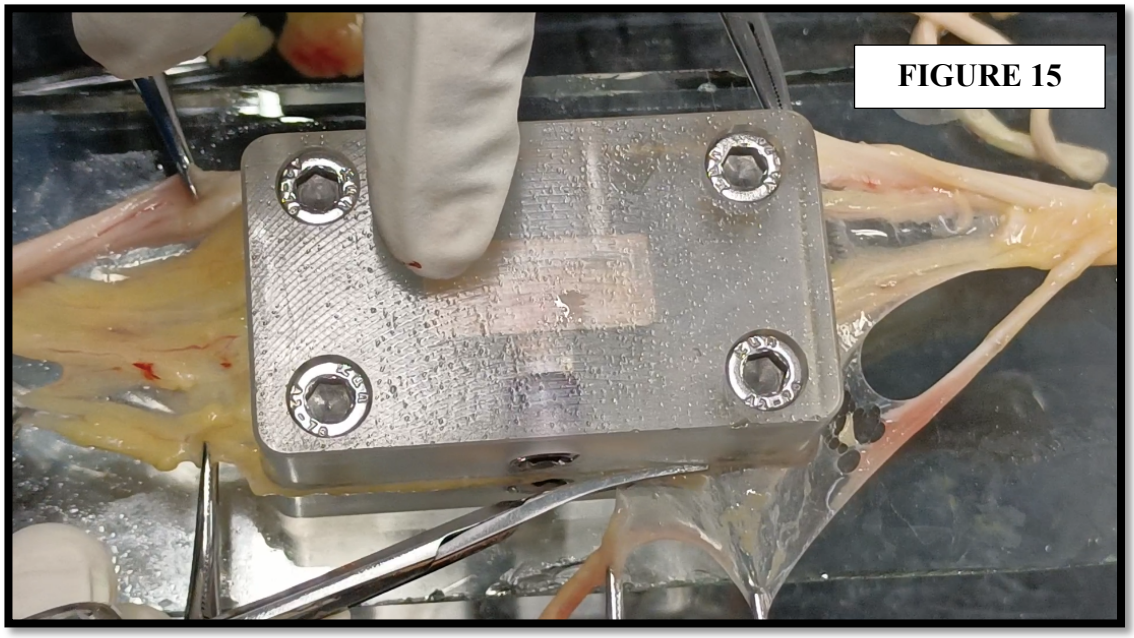

FIGURE 15

Subsequently the Shan-DDC was covered with a waterproof cling drape and then made ready for simultaneous injection of study solutions into both the chambers. The donor and recipient chambers were simultaneously filled with a freshly prepared solution of 1% Lignocaine dissolved in Phosphate buffer saline (PBS) and plain PBS without lignocaine, respectively and the timer was activated. Immediately after the chamber loading, the Shan-DDC was transferred into a temperature-controlled water bath experimental setup, where the temperature was already set at 37 degree Celsius and stirrer speed was set to rotate at 200 revolutions per minute for a period of one hour as described in the experimental set up 5.1.3.1 (section 2) (Figure 16).

FIGURE 16

Using a pre calibrated micropipette, 100 microliters of study samples were drawn from both the donor and the recipient chamber starting immediately after instillation (Time 0) and every 10 minutes till 60 minutes. Thus a total of 14 samples (7 pairs Donor + Recipient), were collected for each paraneural sheath permeability experiment and stored immediately at a temperature of -70°C for further analysis as a batch. To confirm what we have removed was only the Paraneural sheath not the Epineurium of the sciatic nerve 15 pairs of nerve specimens (before and after the removal of the PNS) from 26 sciatic nerves were sent to Histopathological examination and the pathologist confirmed the presence of paraneurium and the epineurium in all the 15 sheathed and de sheathed nerve specimens respectively at a later date (Figure 17).

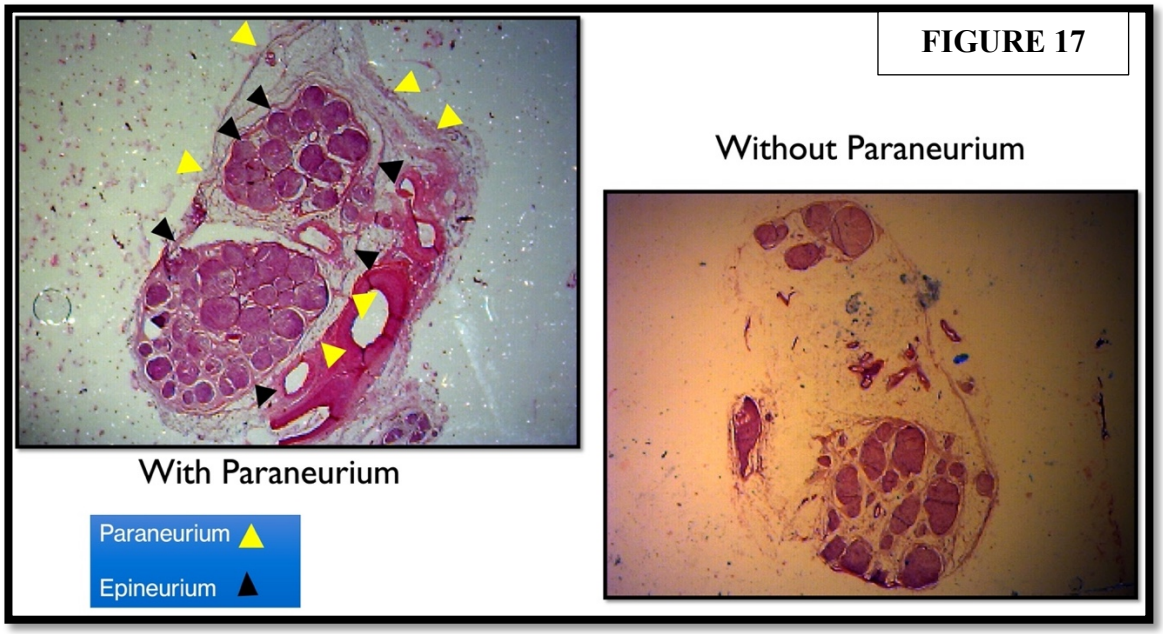

The concentration of Lignocaine in the PBS solution collected from both the donor and recipient chambers was evaluated using an Ultra-Fast Performance Liquid Chromatography (UFLC - Shimadzu, Japan) system linked to a Tandem Mass Spectrometer (Sciex API-4000 MS/MS).

5.2.3 Calculation of Permeability

Flux(Q) was determined by plotting the Lidocaine concentration in the recipient chamber at each time point. The slope of the line relating lidocaine concentration over time data was determined with the use of least-squares linear regression and is equal to the lidocaine flux through 3.36cm^2 paraneural sheath. Then Flux(Q_t) through 1 cm^2 membrane was calculated

by dividing the slope by 3.36cm^2 . Permeability was then determined by rearrangement of the flux equation:

$$\text{Overall Flux } Q_t = P \times [C1 - C2]_t \times A$$

Where:

Q_t = Flux at any given time.

P = Permeability

$[C1 - C2]_t$ = concentration gradient across the paraneural sheath at any given time t (μg/ml).

A = cross sectional area of the paraneural sheath available for diffusion, i.e. area of the port connecting two diffusion chambers which is 3.36cm^2 in Shan-DDC. Since we have already derived Flux per 1 cm square paraneural sheath, permeability at each time interval was calculated by rearranging the Flux equation as follows $P = Q_t / [C1 - C2]_t$. Thus permeability at each time interval (P0, P10, P20…etc) for every paraneural sheath was calculated later average permeability of the individual paraneural sheath was derived. The mean permeability of all the paraneural sheath studied was calculated to know the Lignocaine permeability of human paraneural sheath.

5.3. Estimation of Lignocaine uptake into the human sciatic nerve without the paraneural sheath.

After removal of the paraneural sheath, each sciatic nerve was divided into three segments, each measuring 5 cm in length. Consequently, a 15 cm sciatic nerve from one lower limb yielded three pieces, resulting in 78 sciatic nerve segments collected from 13 individuals for the purpose of conducting 13 nerve experiments. Both ends of each individual nerve segment were securely tied with 3’0 silk (see Figure 18).

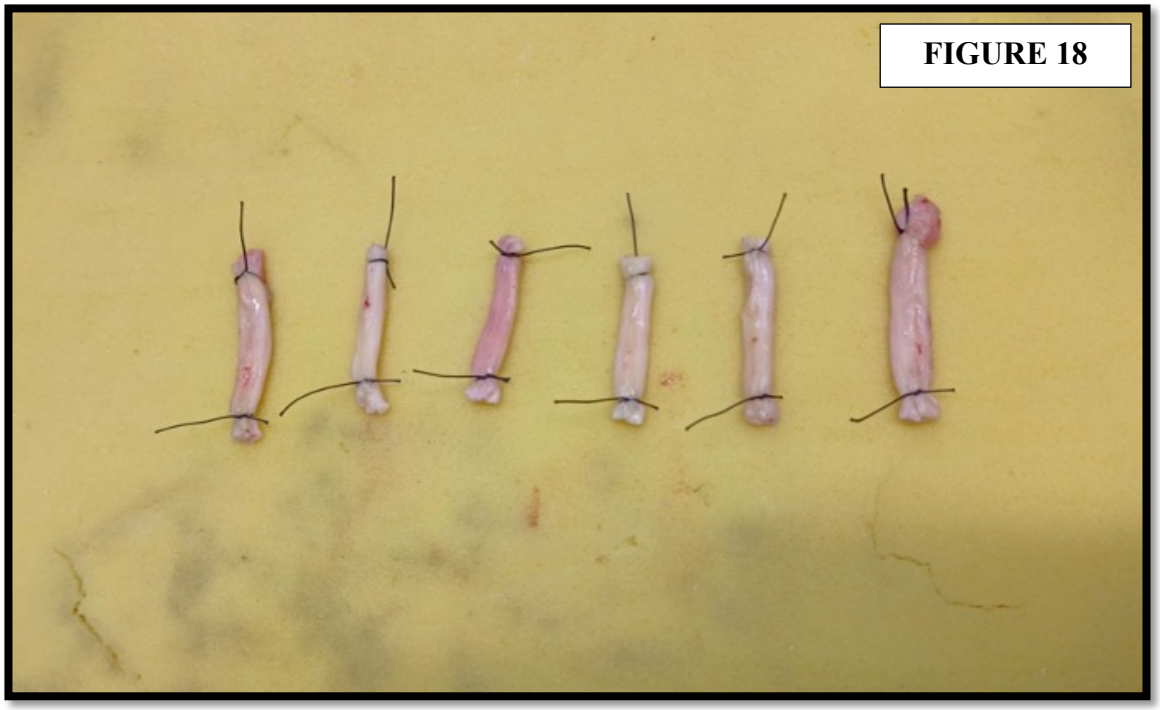

In each experimental setup, six sciatic nerve segments from a single individual were positioned within six microwells, each measuring 40 mm in diameter and 10 mm in depth. The individual nerve segments were anchored diagonally at the edges of the microwells using silk ties at both ends, forming a U-shaped loop at the midpoint of the nerve without touching the bottom of the microwell (Figure 19).

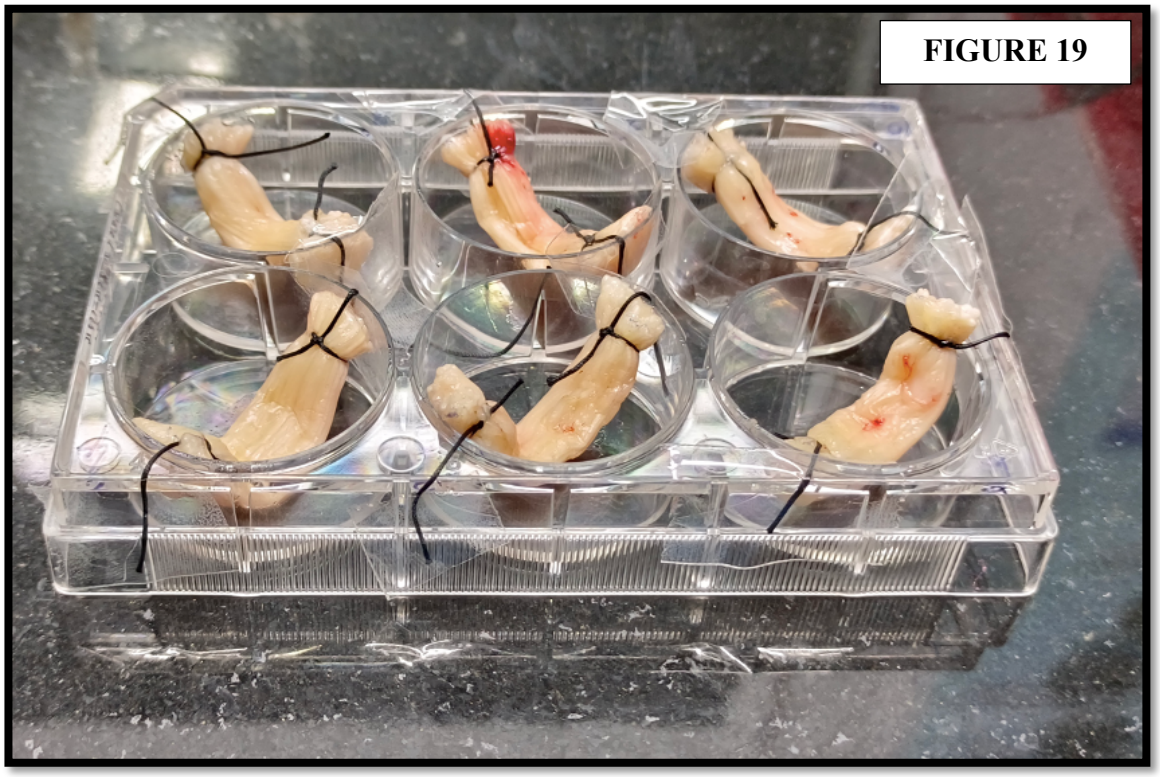

Upon satisfactory anchoring of all six nerve segments, 6 ml of freshly prepared 1% Lignocaine in PBS solution was evenly introduced into all six microwells, ensuring complete immersion of the nerve loops into the local anesthetic solution (Figure 20).

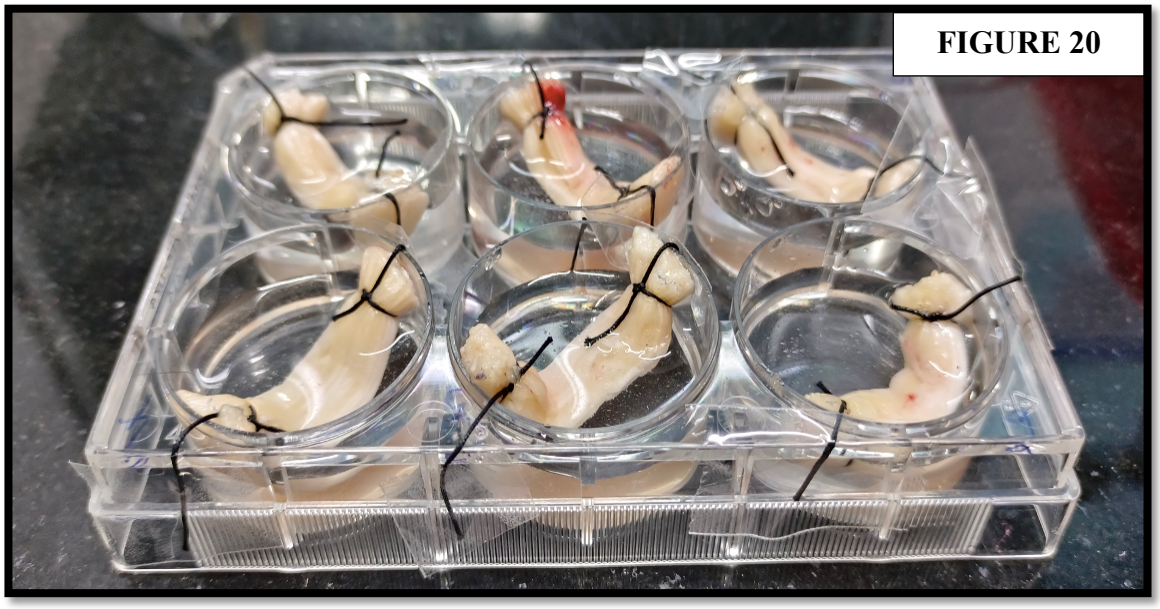

FIGURE 20

Care was taken to ensure that both cut ends of the nerve remained exteriorized and unexposed to the local anesthetic. Subsequently, the timer was initiated. At 10-minute intervals, one nerve segment was removed from the incubation. The nerve loop section immersed in the local anesthetic was excised, properly labelled, and stored at -70°C for subsequent measurement of Lignocaine concentration in the nerve tissue, conducted later as a batch analysis. Additionally, a small piece of sciatic nerve was obtained from the non-soaked excess portion of the sciatic nerve to serve as a control sample for each experiment. Thus, seven nerve samples per experiment (one control without local anesthetic exposure and six nerve samples from the microwells) were collected for subsequent drug analysis (Flow chart). The Lignocaine concentration in the nerve tissue was analyzed using an Ultra-Fast Performance Liquid Chromatography (UFLC - Shimadzu, Japan) system connected to a Tandem Mass Spectrometer (Sciex API-4000 MS/MS).

6. Results

6.1. Demographic data

Twenty six sciatic nerve specimens were removed from 13 diseased individual (8 male and 5 female) aged between 20 to 40 years [mean(SD) 33 ± 6] within 24 hours after their death. Mean (SD) time interval between the reported time of death and the sample harvesting was 14 ± 5hrs. From 26 sciatic nerves 25 paraneural sheath permeability

experiments and 10 nerve uptake experiments could be completed (Flow chart 1). All 35 experiments were completed within 3hours after the sample removed from their respective human body.

Flow chart 1

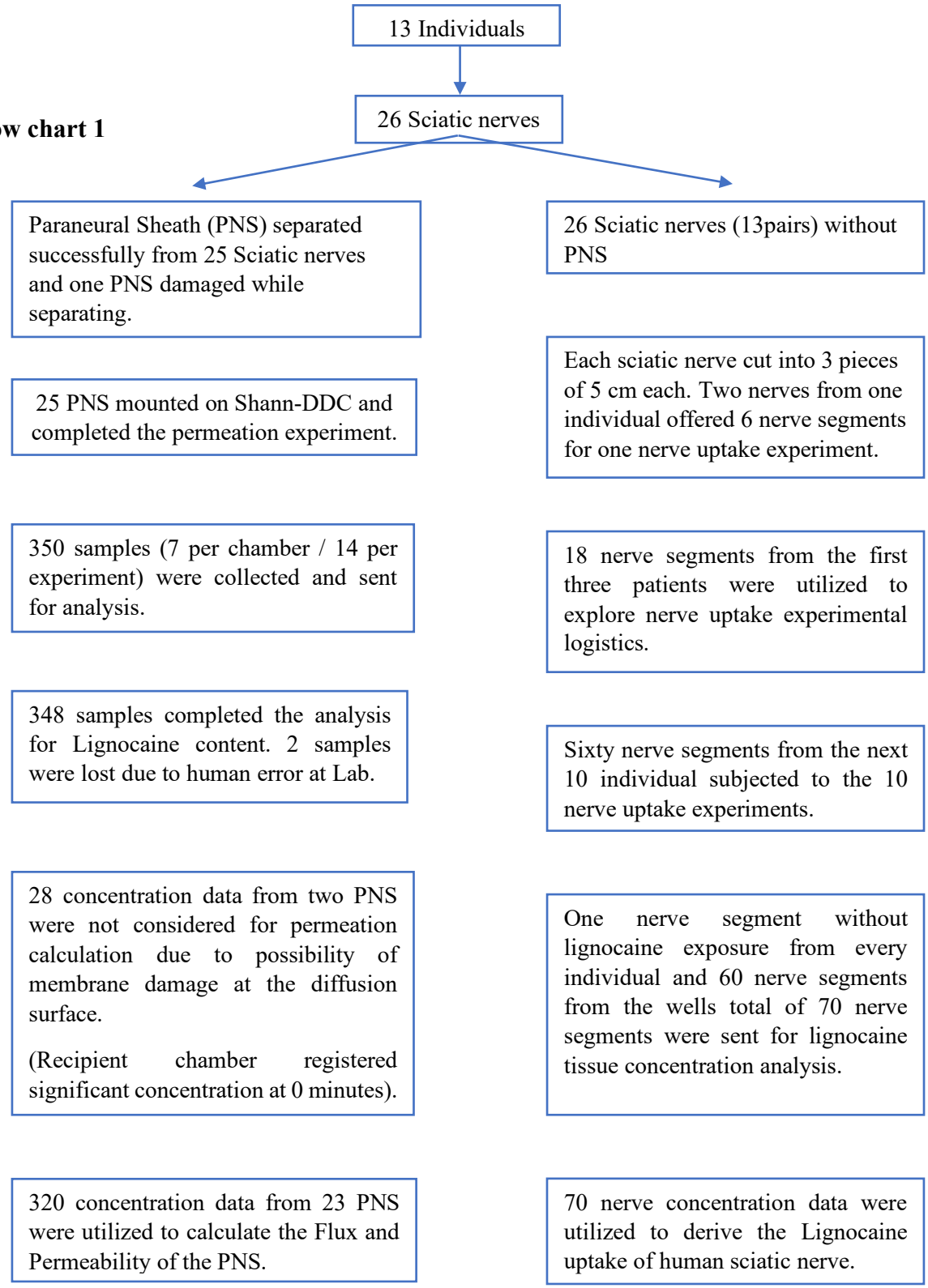
13 Individuals
26 Sciatic nerves
Paraneural Sheath (PNS) separated successfully from 25 Sciatic nerves and one PNS damaged while separating.
26 Sciatic nerves (13pairs) without PNS
25 PNS mounted on Shann-DDC and completed the permeation experiment.
Each sciatic nerve cut into 3 pieces of 5 cm each. Two nerves from one individual offered 6 nerve segments for one nerve uptake experiment.
350 samples (7 per chamber / 14 per experiment) were collected and sent for analysis.
18 nerve segments from the first three patients were utilized to explore nerve uptake experimental logistics.
348 samples completed the analysis for Lignocaine content. 2 samples were lost due to human error at Lab.
Sixty nerve segments from the next 10 individual subjected to the 10 nerve uptake experiments.
28 concentration data from two PNS were not considered for permeation calculation due to possibility of membrane damage at the diffusion surface.
(Recipient chamber registered significant concentration at 0 minutes).
One nerve segment without lignocaine exposure from every individual and 60 nerve segments from the wells total of 70 nerve segments were sent for lignocaine tissue concentration analysis.
320 concentration data from 23 PNS were utilized to calculate the Flux and Permeability of the PNS.
70 nerve concentration data were utilized to derive the Lignocaine uptake of human sciatic nerve.

6.2. Lignocaine permeability of the paraneural sheath

Twenty-five paraneural sheath specimens from 26 sciatic nerves were successfully mounted onto the Shan-DDC, completing 25 permeability experiments. Using pre-calibrated micropipettes, 7 pairs of 100 microliter Phosphate Buffered Saline (PBS) samples were drawn per experiment, resulting in 350 samples that were successfully frozen at -70°C and sent for Lignocaine concentration analysis. The concentration analysis process was detailed in Flowchart 1. Ultimately, 320 concentration data points from 23 paraneural sheaths were included for the analysis of paraneural sheath permeability. Figure 21 depicts the mean (Standard Error of Mean -SEM) Lignocaine concentration (µg/ml) in both the donor and recipient chambers over time.

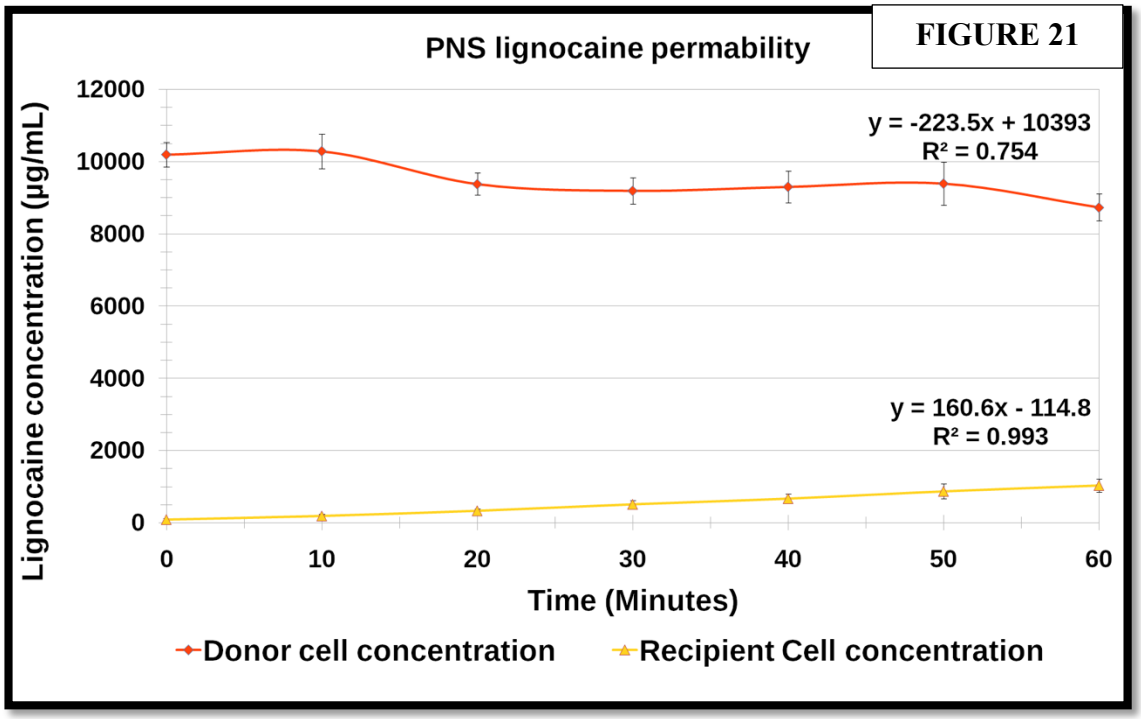

Figure 22 depicts only the recipient chamber concentration over time which indicates 3.36 cm^2 Paraneural sheath allowed 1028 ± 182 µgm/ml (approximately10%) of the Lignocaine to diffuse across at the end of 60 minutes observation period.

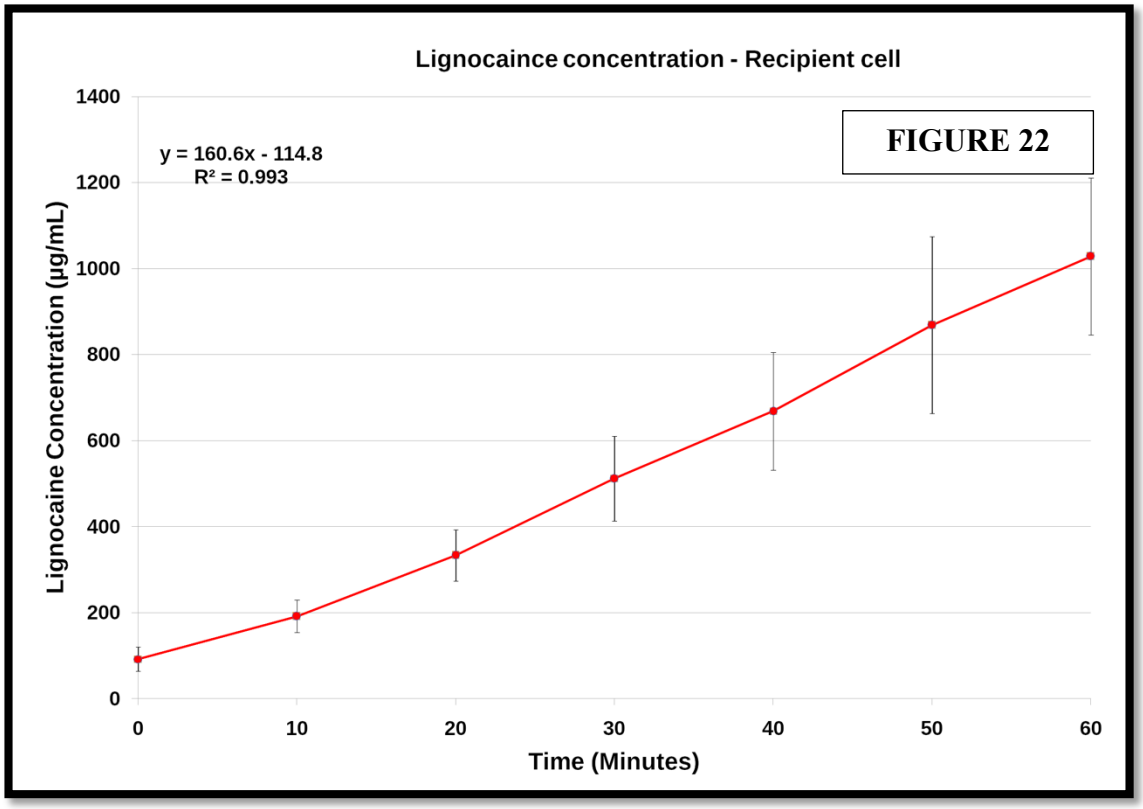

The Mean Flux was 4.78 ± 1.05 µgm/min/cm^2 and the Mean Permeability of the human paraneural sheath was 0.62 ± 0.05 × 10 $^{-3}$ cm/min.

6.3. Lignocaine uptake of human sciatic nerve without the paraneural sheath.

Twenty-six sciatic nerves obtained from thirteen individuals were utilized to provide seventy-eight nerve segments for thirteen nerve local anesthetic (LA) uptake experiments. However, eighteen nerve segments from the initial three patients were allocated for logistical exploration of the experimental setup. Consequently, sixty nerve segments from ten patients were employed to conduct ten nerve Lignocaine uptake experiments. As a result, seventy nerve tissue samples (comprising sixty from microwells and ten baseline samples, one from each individual) underwent analysis for Lignocaine concentration in the nerve tissue. Figure 23 illustrates the mean Lignocaine concentration (SEM) in nmol/mg of wet nerve tissue over the study period. The desheathed human sciatic nerve exhibited a Lignocaine uptake of only 0.046% (1.71 ± 0.21 nmol/mg of wet nerve tissue) of the deposited Lignocaine around the nerve (10 mg/ml Lignocaine = 37 mMol/ml) by the end of the 60-minute observation period.

FIGURE 23

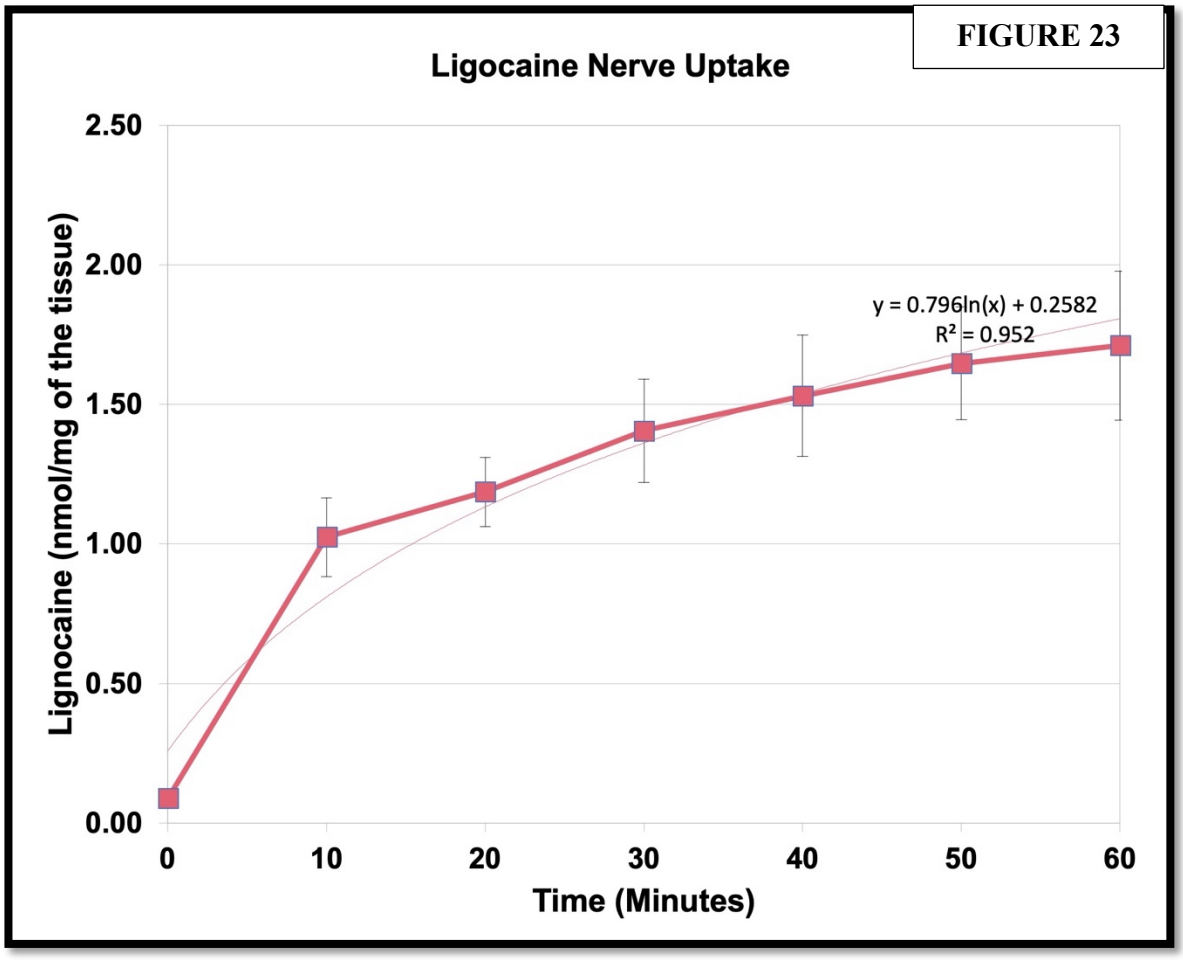

7. Discussion

7.1 Design, development, and validation of Shan-DDC.

7.1.1 Novelty of the design and function of Shan DDC

The size and shape of the diffusion chambers are the defining characteristics of the innovative design of the diffusion cell. These chambers adopt a rectangular shape, with the cuboid (rectangular) form offering the highest surface area to volume (SA/V) ratio among various shapes[34]. The SA/V ratio of the Shan DDC is the highest 0.67 (3.36cm^2/5ml) compared to the other designs such as Moore (0.28)[18], Bernard CM (0.07)[19], McEllistrem (0.60)[16], Grouls (0.02)[24], Rozenn clement (0.07)[25], Karsnov (0.3)[17] and the traditional FDC (0.10). This large surface area allows us to examine the permeability of a greater proportion of biological membranes, particularly in contexts characterized by a high degree of inter-individual variability[35,36], which must be distinguished from equipment and experiment setup-related variability[37]. The longitudinal shape of the diffusion aperture, as opposed to circular designs[16-19], is more aligned with the shape of commonly examined biological

membranes, such as the meninges encircling the spinal cord, sheaths around peripheral nerves, and intimal coverings of the intestines. The 5 ml volume of the recipient chamber, combined with a 3.36 cm^2 surface area for diffusion, provides optimal conditions for testing low permeable substances and yields a minimum of 5 samples (100 microliters each) for testing without the need for replenishment. Unlike the fixed clamp in traditional FDCs, the helical screw thread system in the Shan-DDC offers maximum tightening force to clamp the chambers together, resulting in a negligible leak fraction (1.6%). The larger central stirring well (8 mm diameter over 15 mm surface) at the bottom of both chambers, with a smaller volume of receptor cells (5 ml), ensures optimal stirring performance without vortex formation. Since the sampling port enters the chambers' core from the ceiling, there is no fraction of the unstirred water layer in Shan-DDC as compared to the side arm sampling port of the traditional FDC[38]. Due to the same configurational advantage, the air bubble that forms during sample aliquoting tends to settle in the ceiling and can be readily removed.

7.2 Discussion: Lignocaine permeability of the Paraneural sheath of human sciatic nerve.

7.2.1 The experimental setup and need for invitro settings.

In the context of a typical peripheral nerve block procedure, clinicians administer local anesthetic (LA) in close proximity to nerves. Subsequently, these LA molecules are absorbed by the surrounding tissues, which are more voluminous compared to the nerves themselves. This absorption is accompanied by systemic uptake through adjacent vasculature and diffusion into the peripheral nerve. Consequently, there is a progressive decrease in the concentration gradient across the nerve. Additionally, the pH of the injected LA transitions from its initial acidic state (pH 6.5) to the physiological pH of 7.4 due to the buffering capacity of surrounding tissues and interstitial fluid[39]. Furthermore, both the LA itself and certain adjuvants, such as adrenaline and sodium bicarbonate (CO2), can influence vascular tone, thereby enhancing the removal of drugs from the injection site[40]. Given the dynamic nature of these factors, including the fluctuating concentration gradient, variable surface area exposure, pH gradient, and unpredictable vascular uptake, an in vitro model becomes indispensable for standardizing these parameters to reliably measure the permeability of any perineural connective tissue. Notably, lidocaine remains a commonly studied LA, and 1% (37 mM) is the commonly analyzed concentration still utilized in routine clinical practice[4,5]. The use of phosphate buffer solution as a solvent facilitates the

easy dissolution of lidocaine hydrochloride salt without precipitation, yielding a final stock solution with a pH of 6.85, consistent with previous experimental protocols[5, 24].

7.2.2 Existing data on perineural connective tissue permeability.

Currently, there is a lack of animal or human permeability data concerning any of the perineural connective tissue barriers (Para/Epi/Peri/Endoneurium). However, studies have measured the permeability of the spinal cord meninges for lidocaine in both animal and human tissue models. Human dura-arachnoid membrane showed lidocaine permeability of 17 to 24 × 10^{-3} cm/min at T1 and T12 levels, respectively[24]. In monkeys, the permeability of the dura-arachnoid-pia mater complex was 1.4 ± 0.12 × 10^{-3} cm/min[21]. In contrast, the permeability of the paraneural sheath of the human sciatic nerve was 0.62 ± 0.05 × 10^{-3} cm/min, significantly lower than that of the human dura, indicating that the paraneural sheath (PNS) serves as a significant diffusion barrier for local anesthetics.

Our current understanding of perineural connective tissue barriers is primarily derived from nerve uptake experiments rather than direct permeability measurements, conducted on rat sciatic nerves over the last four decades [4,5,26-28]. Male Sprague–Dawley rats weighing 300–400 g were commonly used in these experiments. The animals were killed at varying stage of laboratory experiments using deep inhalational anaesthesia and the sciatic nerve was dissected in situ from 10mm proximal to sciatic notch to the popliteal fossa, and then excised and frozen in less than 5 s seconds on a flat surface of dry ice [4,5]. The frozen nerve was subsequently desheathed under a dissecting microscope. Authors defined the anatomical structure represented as the sheath in their studies as follows: "we removed the portion of connective tissue and neurovascular bundles around the nerve defined anatomically as the epineurium[41] (referenced back to 1966) and the external portion of perineurium; some of the deeper intraneural part of the perineurium probably remained." As the concept of the paraneurium was not established at the time, authors labeled the removed tissue as epineurium and concluded that perineurium was the main diffusion barrier for intraneural uptake of local anesthetics.

In our present study, we investigated the permeability of the paraneural sheath surrounding the human sciatic nerve, which is well-developed and easily identifiable macroscopically[42]. Ultrasound-guided sciatic nerve block procedures demonstrated that the paraneurium can be separated from the epineurium through hydrodissection[7,11]. However, during microdissection, we observed continuity between the paraneurium and epineurium, requiring serial incisions to separate them. Attempts to incise the epineurium resulted in

the separation and splitting of nerve fascicles. As we could not isolate a sizable epineurium (approximately 3.36 cm^2) from the sciatic nerve, the largest nerve in the human body, we anticipate that the paraneural sheath represents the closest perineural connective tissue whose permeability can be studied in isolation. Histological examination confirmed the presence of epineurium in all desheathed specimens, ensuring that our measurements reflected the permeability of the paraneural sheath of the human sciatic nerve.

7.2.3 Key findings of present research and its correlation with the nerve uptake experiments of animal origin.

The primary findings of this permeation experiment are as follows:

1. The mean flux of lidocaine across the paraneural sheath is 4.78 ± 1.05 µg/min/cm^2.
2. The mean permeability of the human paraneural sheath is $0.62 \pm 0.05 \times 10^{-3}$ cm/min.
3. Only 3% (1028 µg/ml / 3.36cm^2) of lignocaine diffused across one cm^2 of the paraneural sheath at the end of one hour, indicating that the paraneural sheath serves as a significant barrier to the diffusion of local anesthetics.

However, experiments on rat sciatic nerve uptake demonstrated that the penetration of lignocaine into the sciatic nerve (equilibrium uptake) did not differ significantly ($P > 0.05$) with (21.6 ± 3.6 nmol/mg wet tissue) and without (17.2 ± 2.8 nmol/mg wet tissue) the presence of an epineural sheath. However, the uptake was delayed by 50% in the ensheathed nerve (9.1 ± 4.7 min) compared to the desheathed nerve (5.3 ± 2.9 min; $P < 0.02$). Therefore, the authors concluded that while the epineural sheath does not serve as a significant barrier, it does present some obstacle to the entry of lidocaine into the nerve[5].

Contrary to these findings from rat sciatic nerve experiments, clinical experience suggests otherwise. Our previous research demonstrated that the time to readiness for surgery was delayed by 15 minutes, and the duration of analgesia was shorter by 4 hours when the local anesthetic (20 ml, 1:1 mixture of 2% lidocaine and 0.5% bupivacaine) was deposited outside the paraneural sheath of the brachial plexus compared to within the paraneural sheath at the supraclavicular fossa[10]. Similarly, when 20 ml of lidocaine with adrenaline was injected outside the paraneural sheath, the time to complete conduction blockade was delayed by 21 minutes, and the block failed in 30% of patients due to inadequate duration of conduction blockade at the core fibers compared to injection within the paraneural sheath (unpublished data). Similar clinical outcomes were observed in sciatic nerve block by many authors[11], which is consistent with the permeation data of the present study which indicates that the paraneural sheath provides significant impedance to the LA diffusion.

The observed discrepancy between in vitro rat sciatic nerve experimentation data, paraneural sheath permeation findings, and clinical study outcomes may be explained by three key aspects. Firstly, it is crucial to differentiate between tissue uptake and tissue permeation as distinct pharmacokinetic phenomena. Tissue uptake quantifies the amount of drug entering the tissue mass, while permeation assesses the transfer of the drug across specific tissue interfaces, such as partitioning from an aqueous phase into tissue and vice versa. Secondly, concerning tissue uptake, both the nerve and sheath function as a unified entity rather than two separate structures. Experimental evidence[5] demonstrates that under identical incubation conditions, both the sheath and corresponding sciatic nerve exhibit similar levels of lidocaine uptake (equilibrium uptake 49.0 ± 2.9 vs. 43.8 ± 7.2 nmoles/mg wet tissue; $P > 0.05$). Thirdly, in vitro experiments demonstrated that the drug moves across the epineural sheath 50% slower (time constant 5.3 ± 2.9 min) compared to without the sheath (9.1 ± 4.7 min; $P < 0.02$). However, during in vivo situations, as the drug enters the nerve across the para and epineurium, the intraneural vascular network[43] continues to remove a certain fraction of the entered drug molecule. Consequently, the time required to achieve the critical concentration inside the nerve is even more prolonged in the extrafascial injection compared to the subfascial injection (time to complete conduction blockade; 21 vs. 10 minutes; $p < 0.001$) (unpublished data). Notably, this intraneural vascular removal mechanism is absent in vitro, resulting in equivalent equilibrium uptake levels. Nevertheless, in vivo uptake measurements clearly showed that the neural local anesthetic content was significantly lower compared to the in vitro experiments with the same dose of local anesthetic exposure[4,27,32].

7.3. Discussion: Lidocaine uptake of human sciatic nerve without the Paraneural sheath.

7.3.1. key findings and correlation with the existing animal data

Segments of the human sciatic nerve without the paraneural sheath were exposed to freshly dissolved 1% Lidocaine (37mM) in phosphate-buffered saline (pH 6.8) at 22°C for 60 minutes. Every 10 minutes, one nerve segment was removed, and the nerve samples were assayed for Lignocaine content using mass spectrometry. At the end of one hour, the mean Lignocaine content present in the nerve was 1.71 ± 0.21 nmol/mg of wet nerve tissue, amounting to 0.046% of the incubated mass of the drug (37mM). This uptake of 1.71 nmol/mg wet nerve tissue of the human sciatic nerve is far less than the rat sciatic nerve uptake of 43.8 nmol/mg wet. This difference in the uptake of LA inside the nerve could be

due to differences in the experimental setup temperature (22 vs 37°C), ionic composition of the incubating solutions (PBS vs buffered saline), and size of tissue mass, and species difference. Nevertheless, both the animal[4,5] and human tissue data indicate that only less than 2% of the injected or incubated mass of the drug entered the nerve.

7.3.2 Clinical implication of the findings.

Since the experimented human sciatic nerve segments encompassed all three connective tissue layers namely the epineurium, perineurium, endoneurium, and the axonal architecture we were unable to discriminate which component is responsible for the significant resistance to lignocaine diffusion. On the other hand, considering the significant impedance offered by the paraneural sheath, the possibility that all three layers equally contribute to the resistance cannot be dismissed. Hence, the current understanding and teaching of perineurium as the significant diffusion barrier[6] are challenged.

8. Conclusions

8.1. A novel Static Horizontally Aligned Drug Diffusion Cell (Shan-DDC) has been designed, developed, and validated. The horizontally oriented diffusion aperture perfectly aligns with the longitudinal architecture of the paraneural sheath. The highest surface area to volume ratio [0.67 (3.36cm²/5ml)] of the Shan-DDC and less than 5% coefficient variation Lignocaine Flux across cellulose nitrate membrane indicated that Shan- DDC provides reproducible permeation data.

8.2. One cm² of the paraneural sheath of the human sciatic nerve allows only 3% of lignocaine to diffuse across the sheath at the end of one hour. The mean (SEM) flux and permeability of the human paraneural sheath are 4.78 ± 1.05 µg/min/cm² and 0.62 ± 0.05 × 10^{-3} cm/min, respectively, indicating that the paraneural sheath offers significant impedance to LA diffusion.

8.3. The human sciatic nerve without the paraneural sheath takes up only 1.71 ± 0.21 nmol of lignocaine per milligram of wet nerve tissue, which is 0.046% of the incubated LA mass, indicating that neuronal uptake of Lignocaine is extremely low.

References

1. Philip W.H. Peng, Vincent W.S. Anahi Perlas: Minimum effective anaesthetic

concentration of hyperbaric lidocaine for spinal anaesthesia. Can J Anaesth 1998; 45 (2): 122–29.

2. Tran DQ, Dugani S, Correa JA, Dyachenko A, Alsenosy N, Finlayson RJ. Minimum effective volume of lidocaine for ultrasound-guided supraclavicular block. Reg Anesth Pain Med. 2011;36(5):466-9.

3. Franco CD. Connective tissues associated with peripheral nerves. Reg Anesth Pain Med. 37:363-5.

4. Popitz-Bergez FA, Leeson S, Strichartz GR, Thalhammer JG. Relation between functional deficit and intraneural local anesthetic during peripheral nerve block. A study in the rat sciatic nerve. Anesthesiology. 1995 Sep;83(3):583-92.

5. Leeson S, Strichartz G. Kinetics of uptake and washout of lignocaine in rat sciatic nerve in vitro. Anesth Analg. 2013 Mar;116(3):694-702.

6. Lirk P, Hollmann MW, Strichartz G. The Science of Local Anesthesia: Basic Research, Clinical Application, and Future Directions. Anesth Analg. 2018 Apr;126(4):1381-1392.

7. Karmakar MK, Shariat AN, Pangthipampai P, Chen J. High-definition ultrasound imaging defines the paraneural sheath and the fascial compartments surrounding the sciatic nerve at the popliteal fossa. Reg Anesth Pain Med. 2013 Oct;38(5):447–51

8. Sivakumar RK, Karmakar MK, Reina MA, Sala-Blanch X. High-definition ultrasound imaging of the paraneural sheath and fascial compartments surrounding the brachial plexus at the supraclavicular fossa. Reg Anesth Pain Med. 2022 Aug 16;rapm-2022-103822.

9. Areeruk P, Karmakar MK, Reina MA, Mok LYH, Sivakumar RK, Sala-Blanch X. High-definition ultrasound imaging defines the paraneural sheath and fascial compartments surrounding the cords of the brachial plexus at the costoclavicular space and lateral infraclavicular fossa. Reg Anesth Pain Med. 2021 Jun;46(6):500–6.

10. Sivashanmugam T, Ray S, Ravishankar M, Jaya V, Selvam E, Karmakar MK. Randomized Comparison of Extrafascial Versus Subfascial Injection of Local Anesthetic During Ultrasound-Guided Supraclavicular Brachial Plexus Block. Reg Anesth Pain Med. 2015 Aug;40(4):337–43.

11. Perlas A, Wong P, Abdallah F, Hazrati LN, Tse C, Chan V. Ultrasound-guided popliteal block through a common paraneural sheath versus conventional injection: a prospective, randomized, double-blind study. Reg Anesth Pain Med. 2013 Jun;38(3):218–25.

12. Siewert M, Dressman J, Brown CK, Shah VP, FIP, AAPS. FIP/AAPS guidelines to dissolution/in vitro release testing of novel/special dosage forms. AAPS PharmSciTech. 2003;4:E7.

13. Draft Guidance for Industry on Topical Dermatological Drug Product NDAs and ANDAs-In Vivo Bioavailability, Bioequivalence, In Vitro Release and Associated Studies; Withdrawal [Internet]. Federal Register. 2002 [cited 2022 Sep 4].

14. Shivapooja A, Kotla N. The challenges involved in in-vitro drug release testing for semi-solid formulations: advancements and rethinking on various diffusion systems. 2013;6.

15. Bernards CM, Sorkin LS. Radicular artery blood flow does not redistribute fentanyl from the epidural space to the spinal cord. Anesthesiology. 1994;80:872–8.

16. McEllistrem RF, Bennington RG, Roth SH. In vitro determination of human dura mater permeability to opioids and local anaesthetics. Can J Anaesth. 1993;40:165–9.

17. Krasnov VV, Stogov MV, Silant'eva TA, Kubrak NV, Kireeva EA. A Technique for In Vitro Studying of the Permeability of the Spinal Cord Dura Mater. Bull Exp Biol Med. 2018;164:402–3.

18. Moore RA, Bullingham RE, McQuay HJ, Hand CW, Aspel JB, Allen MC, et al. Dural permeability to narcotics: in vitro determination and application to extradural administration. Br J Anaesth. 1982;54:1117–28.

19. Bernards CM, Hill HF. Morphine and alfentanil permeability through the spinal dura, arachnoid, and pia mater of dogs and monkeys. Anesthesiology. 1990;73:1214–9.

20. Bernards CM, Hill HF. The spinal nerve root sleeve is not a preferred route for redistribution of drugs from the epidural space to the spinal cord. *Anesthesiology* 1991;75:827-832.

21. Bernards CM, Hill HF. Physical and chemical properties of drug molecules governing their diffusion through the spinal meninges. *Anesthesiology* 1992;77: 750-756.

22. Bernards CM, Kopacz DJ, Michel MZ. Effect of needle puncture on morphine and lidocaine flux through the spinal meninges of the monkey in vitro. Implications for combined spinal-epidural anesthesia. *Anesthesiology* 1994;80:853-858.

23. Bernards CM, Kern C. Palmitoyl carnitine increases the transmeningeal flux of hydrophilic but not hydrophobic compounds in vitro. Anesthesiology. 1996 Feb;84(2):392-6.

24. Grouls R, Korsten E, Ackerman E, Hellebrekers L, van Zundert A, Breimer D. Diffusion of n-butyl-p-aminobenzoate (BAB), lidocaine and bupivacaine through the human dura-arachnoid mater in vitro. Eur J Pharm Sci. 2000 Dec;12(2):125-31

25. Clément R, Malinovsky JM, Hildgen P, Dollo G, Estèbe JP, Chevanne F, Le Verge R, Le Corre P. Spinal disposition and meningeal permeability of local anesthetics. Pharm Res. 2004 Apr;21(4):706-16.

26. Fink BR, Aasheim G, Kish SJ, Croley TS. Neurokinetics of lidocaine in the infraorbital nerve of the rat in vivo: Relation to sensory block. Anesthesiology. 1975; 42:731–6.

27. Nakamura T, Popitz-Bergez F, Birknes J, Strichartz GR. The critical role of concentration for lidocaine block of peripheral nerve in vivo: Studies of function and drug uptake in the rat. Anesthesiology. 2003; 99:1189–1197.

28. Popitz-Bergez FA, Leeson S, Thalhammer JG, Strichartz GR. Intraneural lidocaine uptake compared to analgesic differences between pregnant and non-pregnant rats. Reg Anesth. 1997; 22:363–371.

29. Bernards, C.M. Human dura mater permeability. Can J Anaesth. 1994; 41:1125.

30. Rosenberg PH, Kyttä J, Alila A. Absorption of bupivacaine, etidocaine, lignocaine and ropivacaine into n-heptane, rat sci- atic nerve, and human extradural and subcutaneous fat. Br J Anaesth 1986;58:310–4 .

31. Strobel GE, Bianchi CP. The effects of pH gradients on the action of procaine and lidocaine in intact and desheathed sciatic nerves. J Pharmacol Exp Ther 1970;172:1-17.

32. Sinnott CJ, Cogswell III LP, Johnson A, Strichartz GR. On the mechanism by which epinephrine potentiates lidocaine's peripheral nerve block. Anesthesiology 2003;98:181–8.

33. Ng S-F, Rouse JJ, Sanderson FD, Meidan V, Eccleston GM. Validation of a static Franz diffusion cell system for in vitro permeation studies. AAPS PharmSciTech. 2010;11:1432–41.

34. Pouran HM. Engineered Nanomaterials in the Environment, their Potential Fate and Behaviour and Emerging Techniques to Measure Them. In: Hussain CM, editor. Handbook of Environmental Materials Management.

35. Turner RM, Park BK, Pirmohamed M. Parsing interindividual drug variability: an emerging role for systems pharmacology. Wiley Interdiscip Rev Syst Biol Med. 2015;7:221–41.

36. Samaras EG, Riviere JE, Ghafourian T. The effect of formulations and experimental conditions on in vitro human skin permeation-Data from updated EDETOX database. Int J Pharm. 2012;434:280–91.

37. Henning A, Schaefer UF, Neumann D. Potential pitfalls in skin permeation experiments: influence of experimental factors and subsequent data evaluation. Eur J Pharm Biopharm. 2009;72:324–31.

38. Miller MA, Kasting G. A measurement of the unstirred aqueous boundary layer in a Franz diffusion cell. Pharm Dev Technol. 2012;17:705–11.

39. Peterfreund RA, Datta S, Ostheimer GW. pH adjustment of local anesthetic solutions with sodium bicarbonate: labora- tory evaluation of alkalinization and precipitation. Reg Anesth 1989;14:265–70

40. Johns RA, DiFazio CA, Longnecker DE. Lidocaine constricts or dilates rat arterioles in a dose-dependent manner. Anesthesiology 1985;62:141–4.

41. Shanthaveerappa TR, Bourne GH. Perineural epithelium: a new concept of its role in the integrity of the peripheral nervous system. Science. 1966 Dec 16;154(3755):1464-7.

42. Andersen HL, Andersen SL, Tranum-Jensen J. Injection Inside the Paraneural Sheath of the Sciatic Nerve: Direct Comparison Among Ultrasound Imaging, Macroscopic Anatomy, and Histologic Analysis. Regional Anesthesia & Pain Medicine 2012;37:410-414.

43. Prahm, C., Heinzel, J., Kolbenschlag, J. (2022). Blood Supply and Microcirculation of the Peripheral Nerve. In: Phillips, J.B., Hercher, D., Hausner, T. (eds) Peripheral Nerve Tissue Engineering and Regeneration.